Groundwater potential assessment leveraging the hybrid objective model (IDOCRIW-CoCoSo) in the basement terrain of Nigeria: insights from remote sensing and geophysical datasets

Kehinde Anthony Mogaji [a], Soliu Ademola Mudashiru [b], Kesyton Oyamenda Ozegin*[c], Sodiq Solagbade Oguntade[d]

[a, b]Department of Applied Geophysics, Federal University of Technology, Akure, Nigeria
[c]Department of Physics, Ambrose Alli University Ekpoma, Edo State, Nigeria
[d]School of Natural and Built Environment, Queen's University Belfast, Belfast, United Kingdom

Authors ORCID IDs: [a]https://orcid.org/0000-0001-7069-1319, [b]https://orcid.org/0009-0003-2305-9646, [c]https://orcid.org/0000-0001-5788-1142, [d]https://orcid.org/0000-0002-6247-1284

*Corresponding author's e-mail: ozeginkess@yahoo.com

Abstract

Groundwater is a valuable asset in both urban and rural areas, where the demand for alternate water sources is increasing—a vital resource for agriculture, industry, and domestic. Assessment of this resource becomes paramount globally and especially in areas where fresh water demand is rising despite falling within a multi-faceted geologic environment—rendering its sustainable management a pressing concern. To address this issue, an Integrated Determination of Objective CRIteria weights–Combined Compromise Solution (IDOCRIW-CoCoSo) was developed by integrating five groundwater potential influencing factors sourced from remote sensing and geophysical datasets. This will increase the prospect of finding productive aquifers and maximize the choice of drilling sites. The results were contrasted with two other hybrid objective modelling approaches, including CRiteria Importance Through Intercriteria Correlation–Combined Compromise Solution (CRITIC-CoCoSo), and Mean Weighted (MW) - CoCoSo. The groundwater potential map produced, classified into five classes, showed that 6% (113 km²), 26% (486 km²), 32% (603 km²), 26% (473 km²), and 10% (192 km²) fall into very low, low, medium, medium high, and high potentiality, respectively. The obtained results were confirmed using the receiver operating characteristic (ROC) curve and sensitivity analysis. According to the area under the ROC curve, the IDOCRIW-CoCoSo had a success rate of 83%, compared to MW- CoCoSo with an area under the curve (AUC) of 75% and CRITIC-CoCoSo (69%). The findings demonstrate IDOCRIW-CoCoSo's higher accuracy in predicting groundwater potential zones. For the sustained development and management of water-scarce areas, this study offers scientific perspective into the sustainability, distribution and governance of groundwater assets.

Keywords: Groundwater; Objective MCDM algorithms; Sustainability; IDOCRIW-CoCoSo; AUC-ROC

.

1. Introduction

Water is an indispensable resource for humanity's advancement (Aneela et al., 2020; Ilugbo et al., 2023a; Ozegin et al., 2023). In the aspect of human development, water serves as the instrument that improves civilizations, fosters agricultural abundance, propels industrial growth, and also underpins the overall well-being of societies at large (Gandy, 2014; Magdoff and Williams, 2017; Barrett et al., 2022). This water, which serves as a vital resource for various aspects of life, can be assessed as both surface water (e.g., visible rivers, lakes, etc.) and water stored beneath the surface of the earth, called groundwater. As Tsur (2018) and Ozegin et al. (2024a) concurred, because of several reasons, including its sustainable yield and lesser proneness to pollution, as well as its purity and reliability, groundwater is preferred to surface water for water exploitation.

In a more geological sense, groundwater is the water that has infiltrated the earth's surface to fill the spaces/voids within sediments and also cracks within rock (Odukoya, 2015; Mogaji and Omobude, 2017; Waltz, 2019). These geologic media, which serve as the storage media for groundwater, are referred to as aquifers. Aside from being the groundwater storage media, the aquifer must also be able to transmit the water in an appreciable quantity for it to be regarded as a rich and good aquifer for groundwater exploitation (Maliva, 2016). Also, in a multi-faceted (complex) geologic setting, the aquifer media are majorly the cracks and fractures within the rocks, contrary to the aquifer media of sedimentary environments, which are the pore spaces within sediments (Aouragh et al., 2017; Mogaji and Omobude, 2017). Furthermore, as highlighted by Ojo et al. (2014), within the complex geologic environment of Nigeria, the aquifers that serve as the groundwater storage media are mainly weathered basement aquifers and fractured basement aquifers. The knowledge of these aquifers has helped researchers to choose efficient research methods (i.e., geophysical approaches, remote sensing, geological approaches, and even interdisciplinary approaches) for studying groundwater potentiality assessment (Shishaye and Abdi, 2016; Mokadem et al., 2018; Fallatah et al., 2019).

According to the estimates of the Food and Agriculture Organization (FAO), by 2025, absolute water scarcity will affect 1.8 billion people, and as a result, water-stress conditions will adversely impact the lives of two-thirds of the world's population at large (Eslamian et al., 2017; Mahato, 2022; Dimkić, 2021). Also, by 2050, the world's population is projected to reach an astonishing 9.7 billion, which will lead to intensifying pressure on agricultural systems, thereby making the swift requirement of more efficient water sources a necessity (Falcon et al., 2022; Giller et al., 2021). These and several other reasons, including climate change, which has also currently been posing a threat to the occurrence of surface water that is paramount for precipitation into the groundwater system, call for efficient and reliable water resource management. As a result, the study of groundwater potentiality assessment is not just an academic exercise but a necessary step towards securing the future of global water resources so that viable water sources can be identified and strategies for sustainable water use can also be developed (Scanlon et al., 2023; Wada, 2016).

Several researchers have highlighted the use of geophysical, remote sensing, and GIS applications for robust groundwater potentiality assessments (Abuzied and Alrefaee, 2017; Mogaji and Lim, 2017; Gaber et al., 2020; Ilugbo et al., 2023a, b; Ozegin et al., 2024b, c). According to their analysis, the framework of combining these approaches ensures a more thorough and robust understanding of groundwater systems. In addition, while the geophysical approach helps in the subsurface characterization and to delineate aquiferous zones, the remote sensing approach provides valuable spatial data on land cover and hydrological conditions, i.e., lineament density, vegetation cover, etc., and the GIS technique facilitates the integration and analysis of these spatial data for informed decision-making as regards the assessment of groundwater potentiality in a particular location (Panahi et al., 2017; Mpofu et al., 2020).

Over the years, the use of multi criteria decision making (MCDM) models has gained extensive recognition in groundwater potentiality assessment studies (Paul et al., 2020; Rahman et al., 2022; Ozegin et al., 2024b, c). Through the use of systematic approaches involving the consideration of various factors that influence decision-making processes, MCDM models have been able to solve the complex nature of decision-making problems related to the

field of groundwater potentiality studies (Arabameri et al., 2020). Several MCDM models have been applied for the decision-making process in groundwater potentiality studies, notably the analytical hierarchy process (AHP) (Adeyemo et al., 2017; Akinlalu et al., 2017; Ozegin et al., 2024a, b, c), evidential belief functions (Al-Abadi, 2017; Nair et al., 2017), and the Preference Ranking Organization method for enrichment evaluation (PROMETHEE II) (Roozbahani et al., 2017; Mogaji et al., 2022). As reported in the literature (Elubid et al., 2020; Farhat et al., 2023), although the approach involving the use of a single MCDM model provides good results in relation to groundwater potentiality assessment, due to their ability to enhance the accuracy of the potentiality assessment, researchers have recently shifted towards the adoption of combined MCDM models (Dey et al., 2021; Farzin et al., 2021; Karakuş, 2023). In this approach of combined MCDMs, comprehensive analysis is being performed by leveraging the strengths of multiple decision-making techniques. As found in several pieces of literature, combined MCDMs may stem from the approach of assigning weights to the influencing factors with one model and ranking the alternative with the other model: TOPSIS-Entropy (Atenidegbe and Mogaji, 2023), AHP-TOPSIS (Pathan et al., 2022), PROMETHEE-Entropy (Mogaji and Atenidegbe, 2023), or through the combination of fuzzy logic with another MCDM model: fuzzy-AHP (Radulović et al., 2022) and fuzzy-TOPSIS (Adiat et al., 2024). On the other hand, machine learning (ML) models have been proven to be effective in groundwater assessments, as analyzed by multiple scholars (Dewey and DeVries, 2021; Dixit et al., 2020; Hiyama and Omodaka, 2021); however, they are usually unsuitable in validation data-sparse regions. The lack of adequate data for training is the main drawback to using machine learning (Iluore et al., 2025). For instance, the study area only had sparse actual borehole yield data available for validation. The adopted approach in this present study thus offers a more reliable alternative in terms of objectivity and a data-driven approach even with the limited data, making it more suitable in this context.

MCDMs such as Integrated Determination of Objective CRIteria Weights (IDOCRIW), CRiteria Importance Through Intercriteria Correlation (CRITIC), Mean Weighted Model (MWM), and Combined Compromise Solution (CoCoSo) have proven useful for extensive decision-making processes in various specialties (Alao et al., 2021; Eslami et al., 2021; Luo et al., 2021; Popović, 2021; Shi et al., 2021; Şahin, 2021). IDOCRIW is an objective weightage-determining framework that incorporates the entropy model and Criterion Impact LOSs (CILOS) for enhancing objective weighing of criteria (Ayan et al., 2023). While the CRITIC framework determines objective weight to criteria based on their differing characteristics (Hashemkhani Zolfani, 2024), MWM assigned equal objective weight to the criteria (Sahin, 2021). Conversely, the CoCoSo method, is predicated on a combined exponential basis weighted output model with "simple additive weighting (SAW)." Considering assessing groundwater potential necessitates methodological frameworks capable of incorporating a variety of parameters, three modelling approaches were chosen for this study: Integrated Determination of Objective CRIteria weights–Combined Compromise Solution (IDOCRIW-CoCoSo), CRiteria Importance Through Intercriteria Correlation–Combined Compromise Solution (CRITIC-CoCoSo), and Mean Weighted-CoCoSo.

The IDOCRIW-CoCoSo model represents a novel approach with limited application in groundwater potential assessment. It effectively combines IDOCRIW weighting with CoCoSo, thereby addressing both variability and intercorrelation among the criteria. Recent research studies indicate that hybrid approaches combining objective weight with robust ranking in multi-criteria decision-making (MCDM) surpass traditional aggregation methods (Bhaskar and Khan, 2022; Petrović et al., 2023; Sahoo and Goswami, 2023). The CRITIC-CoCoSo model was used for comparing the proposed approach. This method assigns weights objectively using the CRITIC model, providing an independent baseline against which to test the IDOCRIW (Hassan et al., 2023). Finally, we built the Mean Weighted- CoCoSo model to determine whether performance increases are mostly due to the weighting technique or the CoCoSo aggregation operator itself. The study uses these model suites to ensure a full examination of objective and equal weighing techniques, as well as aggregation procedures. Leveraging on the insights of Jitta et al. (2025), such a comprehensive comparison approach allows for the most accurate identification of the suggested model's methodological superiority.

The study area falls within the Southwestern basement complex geology of Nigeria, where, due to the multi-faceted geologic nature, groundwater potentiality assessment involves a complex process that requires precision and higher accuracy in the decision-making process (Mogaji and Atenidegbe, 2023; Osinowo and Arowoogun, 2020). In addition, increases in population, urbanization, and agricultural activities within several parts of this southwestern region have made the demand for potable water skyrocket, ultimately requiring efficient groundwater potentiality

assessment (Ayejoto et al., 2023; Adeolu, 2019). In view of this, the aim of this present study is to explore the novel approach of applying the IDOCRIW-CoCoSo objective modelling algorithm for robust, efficient, and accurate groundwater potential assessment in the study area. Furthermore, the validated result of the model is expected to be used for informed decision making as related to groundwater resource management of the study area. Additionally, the methodological processes developed can also be adopted in regions with similar geology.

2. Material and methods

2.1 Study area

2.1.1 Location, accessibility, climate and vegetation

The study area is located within the northern part of Ondo State, southwestern Nigeria. It is bounded within longitude 4°50'0"E to 5°40'0"E and latitude 6°55'0"N to 7°25'0"N. The study area has an area coverage of 1869 square kilometres and cuts across five local governments within the northern part of Ondo State, namely, Ondo East, Ile Oluji, Ifedore, Akure South, Akure North, and parts of Owo. The study area exhibits diverse geography throughout the towns that fall within it. There is a gradual shift in elevation above sea level ranging from above 300 m for towns including Moferere and Fagbo, which are all located in the southwestern part of the study area, to the highest elevation areas above 600 m, which fall to the northern part of the study area, including Ijare, Iju, and Igbara Oke (Akinluyi et al., 2018; Imeokparia and Falowo, 2020; Olajide et al., 2020) (**Fig. 1**). Furthermore, the rainy season in the study area occurs from April to October and is characterized by substantial downpour, ranging from 1,150 to 2,000 mm per year, while in the dry season, which occurs from November to March, the temperature ranges from 25°C to 29°C, with the dry season also including the arrival of the harmattan season (Omonijo and Matzarakis, 2011). The vegetation of the study area is forest-savannah.

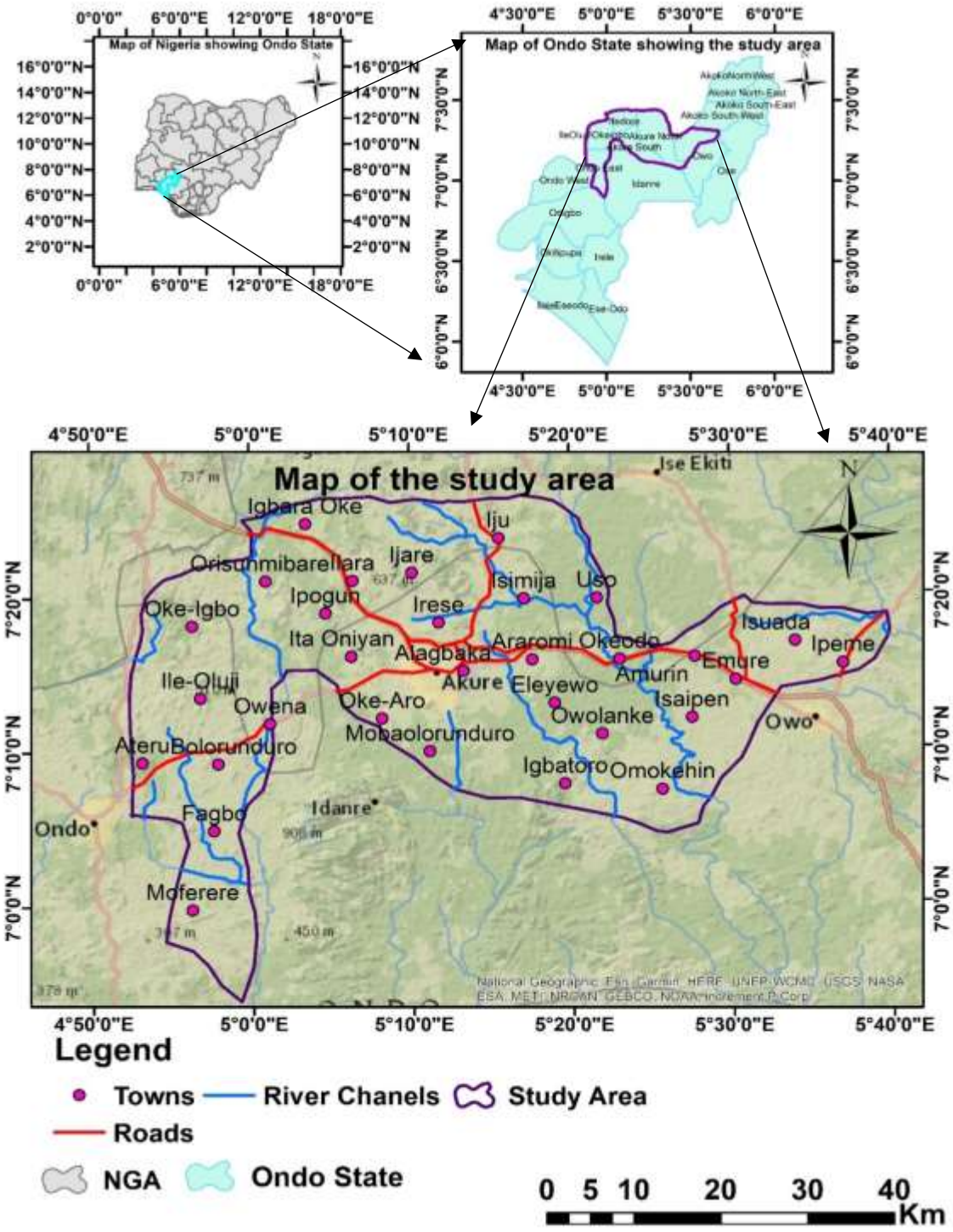

Fig.1. Location map of the study area showing inset map of Nigeria and Ondo State

2.1.2 Hydrogeology of the study area

The study area, which is located within the northern part of Ondo State and also includes some parts of Owo, falls within the Precambrian basement complex. According to the analysis of several researchers (Idris *et al.,* 2018; Adeoti and Okonkwo, 2016), these rocks are hard, compact, and crystalline and thus, possess low primary porosity. These make groundwater occurrence within them to be heavily reliant on secondary porosity and permeability, which are primarily influenced by weathering and structural features within the rock types (Akinwumiju and Olorunfemi, 2019). Weathering processes, fracture systems, and structural features such as lineaments and joints all play a crucial role in enhancing groundwater storage in the Basement Complex terrains. In the study area, as modified from the Nigerian Geological Survey Agency (NGSA) map, the five major rock units/lithologies observed are Migmatite gneiss, Older granite, Porphyritic Granite, Granite gneiss, and Biotite Granite (**Fig. 2**).

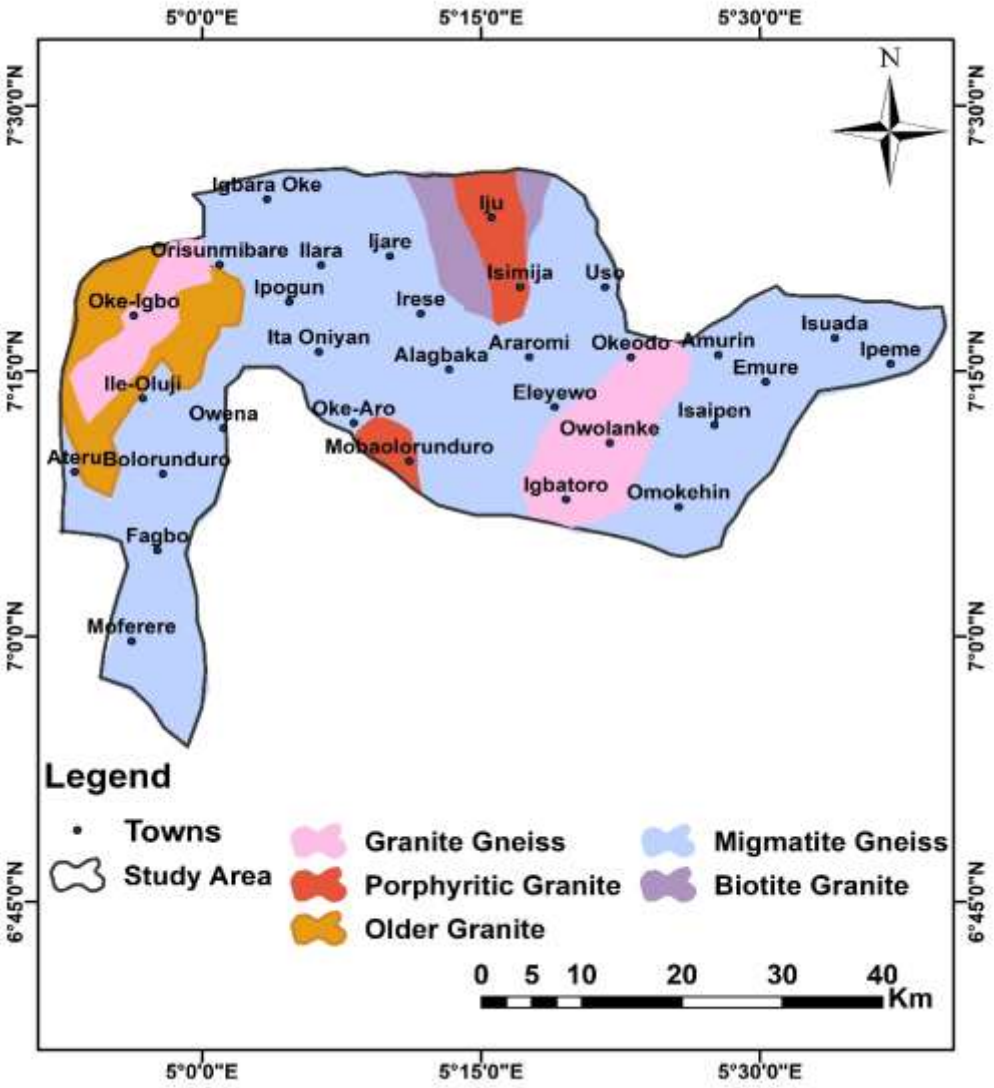

Fig. 2. Geologic Map of the Study Area, modified after NGSA (1996)

2.2 Data sources

2.2.1 Remote sensing data

The remote sensing data employed in this study include Digital Elevation Model (DEM) datasets, Sentinel 2 Data, and Moderate Resolution Imaging Spectroradiometer (MODIS) datasets. The DEM of the study area was obtained from satellite imagery employing Shuttle Radar Topography Mission (SRTM), which has a 30 m resolution and was accessed from the OpenTopography website (*portal.opentopography.org*) as well as from the USGS Earth Explorer website (*earthexplorer.usgs.gov*). Sentinel 2 data was accessed from Environmental Systems Research Institute (ESRI) Sentinel 2 20m Global Land Use Land Cover data (*https://www.arcgis.com/apps/instant/media/index.html*). The MODIS dataset was accessed from NASA Level-1 and Atmosphere Archive & Distribution Systems Distributed Active Archive Centre (LAADS DAAC) (*https://ladsweb.modaps.eosdis.nasa.gov/search/*). The study's geophysical and remote sensing datasets are shown in **Table 1.**

Table 1. Details of the data sources from which GPCFs thematic layers were extracted

GPCFS thematic layers	Data source	Study area coverage	Period
Land Use/Land Cover (LULC)	ESRI Sentinel 2 Global land use/land cover with 10m resolution	Full coverage	April 18, 2023
Normalized Difference Vegetation Index (NDVI)	MODIS13Q1 datasets from NASA LAAD DAACS with 250 m resolution	Full coverage	March 5, 2023
Coefficient of Anisotropy (COA)	VES data from an electrical resistivity geophysical survey	Dense coverage	2015 - 2017
Transmissivity (T)	VES data from an electrical resistivity geophysical survey	Dense coverage	2015 - 2017
Transverse Resistance (TR)	VES data from an electrical resistivity geophysical survey	Dense coverage	2015 - 2017

2.2.2. Geophysical Data

The electrical resistivity (ER) assessment aims to estimate the subsurface resistivity distribution by taking evaluations on the earth's surface. The ER approach was used in this study to evaluate the geohydraulic response characteristics of the aquifer components in the study location (Eze et al. 2022; Ilugbo et al. 2023). For this study, the ER method involves the use of the vertical electrical sounding (VES) technique with the Schlumberger array. A maximum electrode spacing of 200 m was espoused. Two hundred and fifty (250) VES data were collected in the entire study area to ensure well-distributed data (**Fig. 3**). The resistivity meter assessed the potential difference established in the subsoil, and the procedure continued by extending the distance between the current electrodes proportionately from the midway. Expanding the interval between the potential electrodes was handled with caution, ensuring that the potential field wasn't weak, which was accomplished by ensuring that the space between the potential electrodes wasn't greater than one-fifth of the separation between the current electrodes (Loke and Barker, 1996; Egbeyale et al. 2022; Eze et al. 2022; Ikpe et al. 2022; Mudashiru et al., (2024); Ilugbo et al. 2023; Fajemilo, and Ozegin, 2025). As a measure of caution, the profiling lines were kept straightened, and measurements were not acquired within the electric cables to prevent unwanted electromagnetic waves that could alter the data. The data were mechanically smoothened, eliminating outliers at the crossing distance that did not correspond to the geology of the investigated areas (Eze et al. 2022). Though the analysis of the gathered data was influenced by ground truth

data, the outcomes of the study were quantitatively shown to be consistent with data from comparable geology within as well as beyond the research area.

The acquired data were subjected to a partial curve matching technique, after which computer iterations using WinResist Version 1.0 software were then used to generate the depth sounding curves (**Figs. 4a-d**). Additionally, analysis was performed for determining the curve types (**Fig. 5**), inferred geoelectric layers (**Table 2**), and first-order geoelectric parameters, as well as the second-order geoelectric parameters, which are all essential to compute the values for the GPCFs derived from the geophysical datasets.

Eq. (2) is used to calculate the geometric factor (K) for the Schlumberger array ((Loke and Barker, 1996; Eze et al. 2022; Idiahi et al. 2023)

$$K = \left[\left(\frac{AB}{2}\right)^2 - \left(\frac{MN}{2}\right)^2\right] \times \pi \qquad (2)$$

With AB representing the current electrode spacing, MN for the potential electrode spacing, and $\pi = \frac{22}{7}$.

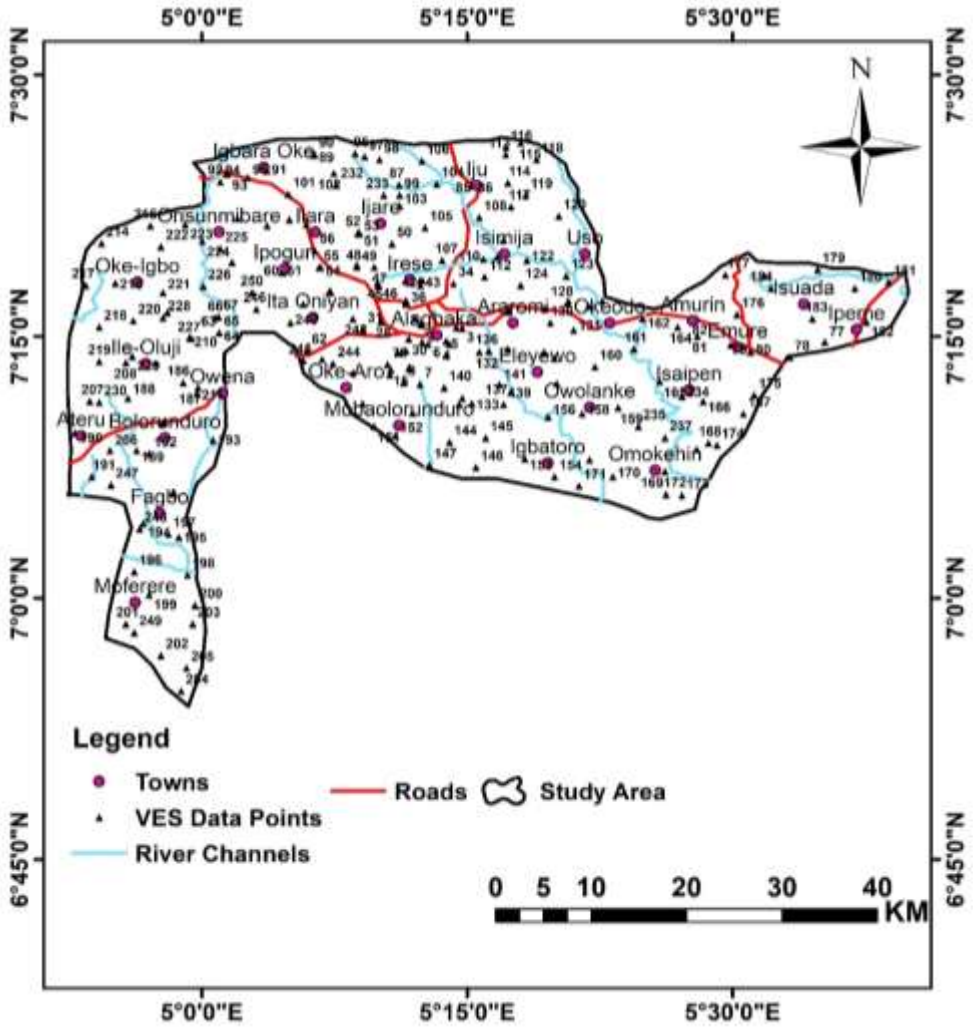

Fig. 3. VES data acquisition map of the study area

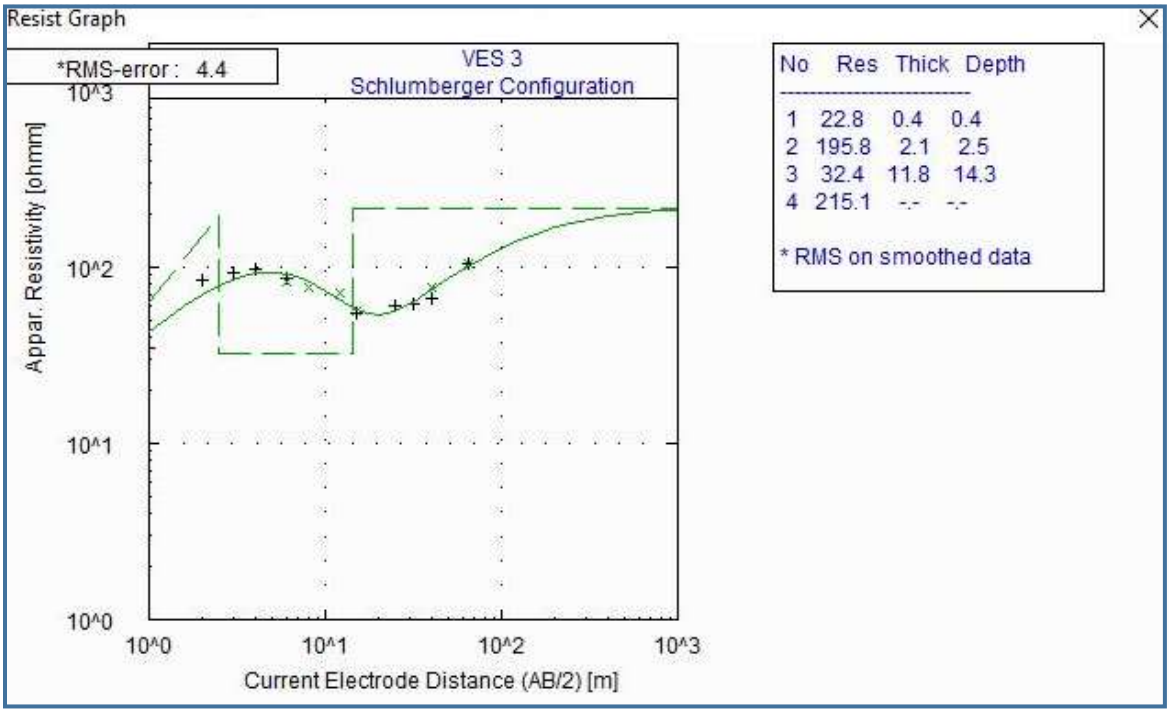

Fig.4a. KH Curve type delineated in the study area

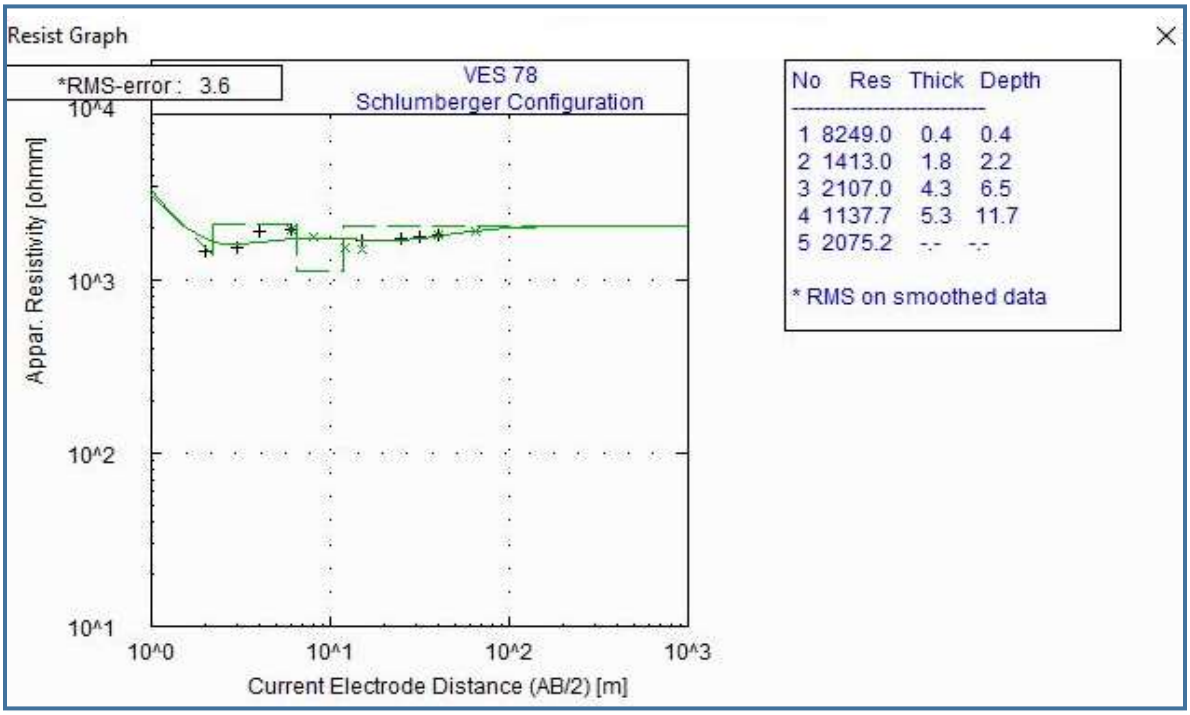

Fig.4b. HKH Curve type delineated in the study area

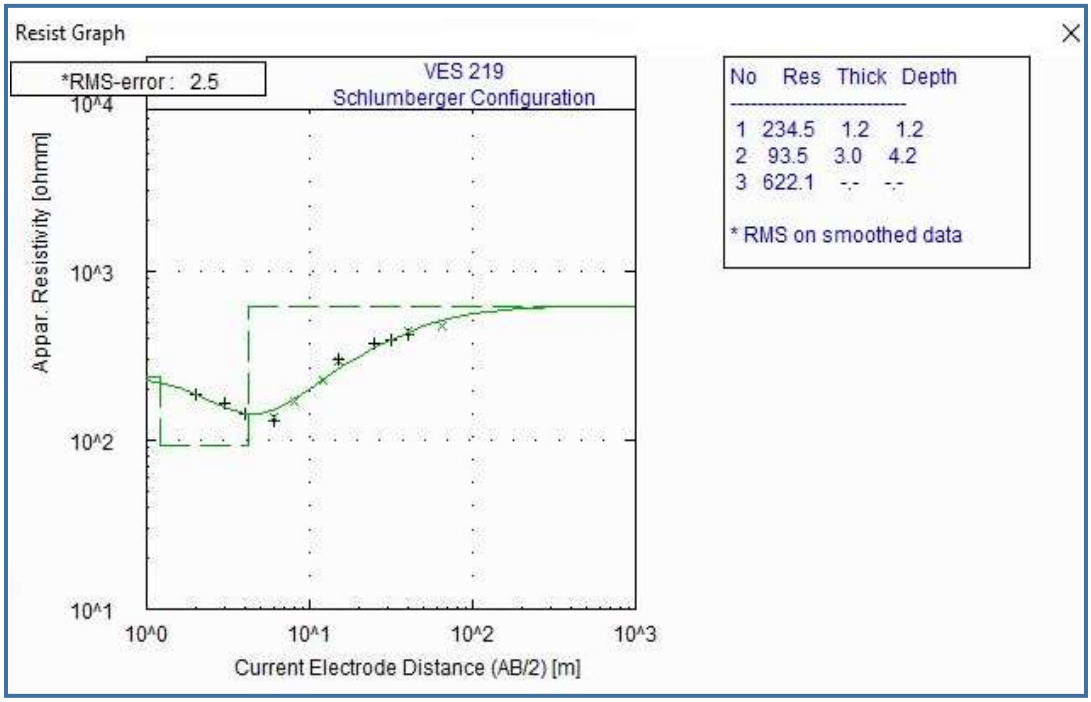

Fig.4c. H Curve type delineated in the study area

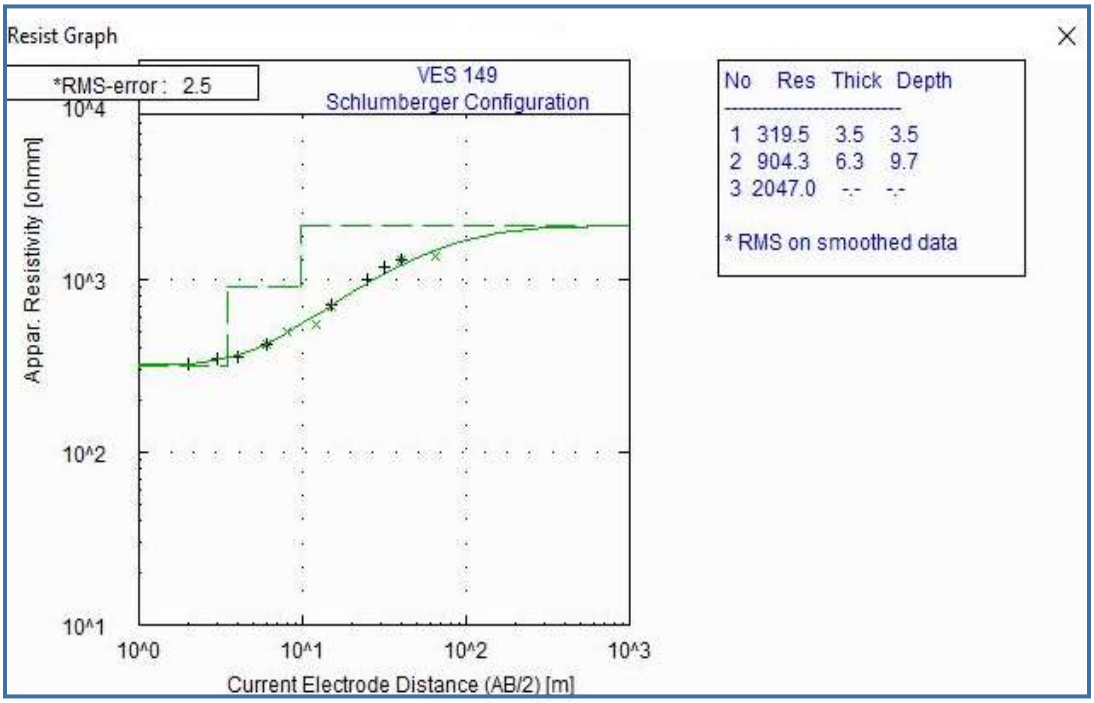

Fig.4d. A Curve type delineated in the study area

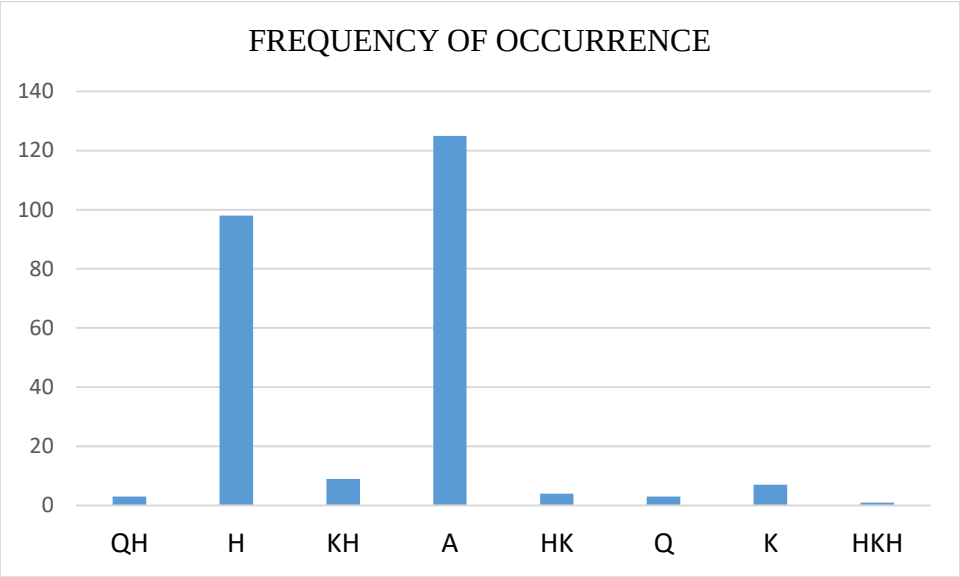

Fig. 5. Curve type frequency of occurrence within the study area

2.3 Groundwater Potential Conditioning Factors (GPCFs)

As asserted by several researchers (Das and Pardeshi, 2018; Maity and Mandal, 2019; Benjmel et al., 2022), the groundwater potentiality of a region, particularly a multifaceted geologic environment, is influenced by numerous factors. In this present study, land use/land cover (LULC), normalized difference vegetation index (NDVI), transmissivity (T), transverse resistance (TR), and coefficient of anisotropy (COA) selected from remote sensing and geophysical datasets were the GPCFs considered. In addition, this literature (Mogaji and Lim, 2017; Kanagaraj et al., 2019; Kamali et al., 2020; Nag et al., 2022; Konwea et al., 2023) has highlighted the relevance of the selected GPCFs on the assessment of groundwater potentiality of a particular region. Furthermore, the following subsections elaborate further on the relevance of these selected GPCFs.

2.3.1Land Use/Land Cover (LULC)

Land use/land cover (LULC) refers to the physical characteristic and purpose of the land, including its natural and artificial features (Liaqat *et al.*, 2021). As related to groundwater potentiality assessment, different land cover types exhibit varying levels of permeability, which influences the level of infiltration and groundwater recharge (Arunbose *et al.*, 2021). While urban areas with impervious surfaces such as concrete and asphalt limit water infiltration, thereby leading to reduced groundwater potential, vegetated and permeable surfaces enhance infiltration, which ultimately leads to increased groundwater potential (Kuruppu *et al.*, 2019). For this study, the LULC data was obtained from ESRI Sentinel 2 Global Land Use Land Cover data (*https://www.arcgis.com/apps/instant/media/index.html*).

2.3.2 Normalized Difference Vegetation Index (NDVI)

NDVI is a metric that assesses the relative abundance of green vegetation in a given area (Robinson et al., 2017). It is estimated by analyzing the red and near-infrared (NIR) bands of radiation from the sun reflected from the object. NDVI is computed using **Eq.1.**

NDVI = (NIR - Red) / (NIR + Red) (1)

NDVI generally ranges from -1 to +1, with values closer to 1 indicating greater vegetation density, while values closer to -1 indicate less vegetation density. As Bhunia (2020) and Ozegin and Ilugbo (2025) point out, high NDVI values in a given area indicate healthy and thick vegetation, implying high infiltration rates. As a consequence, higher NDVI values correspond to larger infiltration areas and greater groundwater potential; however, lower NDVI values correspond to smaller infiltration areas and consequently lower groundwater potential. For this study, NDVI MODIS13Q1 data was accessed from NASA Level-1 and Atmosphere Archive & Distribution Systems Distributed Active Archive Centre (LAADS DAAC) (*https://ladsweb.modaps.eosdis.nasa.gov/search/*).

2.3.3 Coefficient of Anisotropy (COA)

COA is a dimensionless second-order geophysical parameter calculated from the transverse resistivity and longitudinal resistivity. COA shows the degree to which the subsurface lithology is inhomogeneous (George et al., 2020). The heterogeneity measured by COA may result from fracturing or weathering, which are necessary for secondary porosity (Akintorinwa et al., 2020). This secondary porosity is higher with increasing COA, which ultimately indicates that areas having higher COA will experience higher groundwater potentiality and vice versa (Akinlalu et al., 2022).

In this study, COA is calculated using **Eqs. 2–5**;

$$COA = \sqrt{\frac{p_{TR}}{p_{LC}}} \quad (2)$$

$$p_{TR} = \frac{TR}{H} \quad (3)$$

$$P_{LC} = \frac{H}{LC} \quad (4)$$

by substituting eq. 3 and eq. 4 into eq. 2, the final formular of COA is,

$$COA = \sqrt{\frac{TR}{H} \times \frac{LC}{H}} = \frac{\sqrt{TR \times LC}}{H} \quad (5)$$

where ' p_{TR} ' is the average transverse resistivity (Ωm^2), ' P_{LC} ' is the average longitudinal resistivity (Ωm^2), 'TR' is the total transverse resistance (Ωm^2), 'LC' is the total longitudinal conductance (mhos), 'H' is the thickness of the overburden materials (m), 'COA' is the coefficient of anisotropy.

2.3.4 Transmissivity (T)

Transmissivity (T) is referred to as the rate at which water flows through a unit width of the aquifer thickness under a unit hydraulic gradient (Hasan et al., 2018). In essence, T, which is also a second-order geoelectric parameter, measures the ease with which fluid moves through an aquifer and is the product of the aquifer thickness (h) and hydraulic conductivity (HC). As analyzed by Mallick et al. (2019), areas with higher transmissivity can transmit water more readily, allowing for higher pumping rates, thus suggesting that such areas will have higher groundwater potential and vice versa.

In this study, T was calculated using **Eq. 6**;

$$T = h \times HC \quad (6)$$

Where 'h' is the aquifer medium thickness (m), 'HC' is the hydraulic conductivity (m/day) given by HC = 0.0538exp(-0.0072ρ) and modified from the hydraulic equation presented by Mogaji and Atenidegbe (2023); k = 0.0538exp(-0.0072ρ) where 'ρ' is the aquifer layer resistivity, 'T' is the transmissivity (m^2/day)

2.3.5 Transverse Resistance (TR)

Transverse resistance (TR) is also a second-order geo-electric parameter that refers to the ease of groundwater flow to the aquifer perpendicular to the groundwater flow (Hassan et al., 2017). Transverse resistance (TR) is calculated as the summation across all the overburden layers of the product of the layer thickness (h) and the layer resistivity (ρ). According to Hasan et al. (2018), TR has been found to be directly related to transmissivity (T), which suggests that areas with higher TR values will experience higher groundwater potential since such areas will be able to transmit water readily and vice versa.

In this study, TR was calculated using **Eq. 7**;

$$TR = \sum_{i=1}^{n} h_i p_i = h_1 p_1 + h_2 p_2 + ... + h_n p_n \quad (7)$$

where 'h' is the layer thickness (m), 'ρ' is the layer resistivity (**Ω**), 'n' is the number of layers, and 'TR' is the transverse resistance (**Ω**m^2)

Table 2 shows a summary of the interpreted geoelectric result from some of the VES data.

All GPCFs thematic maps (**Figs. 6a–10a**) were generated using ArcGIS 10.7 software. Furthermore, the pie charts (**Figs 6b-10b**) show the area coverage of each class within each thematic layer, and for the pie charts, the abbreviations explaining the area coverage are VL (very low), L (low), M (medium), MH (medium-high), and H (high). Figures 6a–10a and 6b–10b are shown in the **appendix**.

Table 2. Summary of interpreted geoelectric result from VES data

VES no	Layer Resistivity (Ωm)	Layer thickness (m)	Curve Type	Infered geoelectric layers	Inferred existence of aquifer layer
	$\rho_1/\ \rho_2/\ \rho_3/\ \rho_4/\ \rho_5$	$h_1/h_2/\ h_3/\ h_4$			
1	606/170/26/339	0.5/12.4/7.8	QH	Top soil/Weathered layer/Fractured basement/Basement	Present (Layer 3)
2	536/181/779	1.3/10.2	H	Top soil/Weathered layer/Basement	Present (Layer 2)
3	65/207/37/481	0.7/3/6.2	KH	Top soil/Weathered layer/Fractured basement/Basement	Present (Layer 3)
4	603/1245/2190	2.6/9	A	Top soil/Weathered layer/Basement	Not present
5	114/54/815	2.1/6.6	H	Top soil/Weathered layer/Basement	Not present
50	10/222/394	0.6/9.9	A	Top soil/Weathered layer/Basement	Not present
100	250/384/1510	2.2/11.1	A	Top soil/Weathered layer/Basement	Present (Layer 2)
200	230/572/959	1.2/9	A	Top soil/Weathered layer/Basement	Not present
246	584/157/1775	1.3/7.7	H	Top soil/Weathered Layer/Fresh basement	Present (Layer 2)
247	164/490/729	1.9/10.5	A	Top soil/Weathered layer/Basement	Not present
248	69/526/815	1.6/7.8	A	Top soil/Weathered layer/Basement	Not present
249	509/188/491	2.2/9.7	H	Top soil/Weathered layer/Basement	Present (Layer 2)
250	358/193/751	2/10	H	Top soil/Weathered layer/Basement	Present (Layer 2)

2.4 The adopted multi-criteria decision-making (MCDM) models

This section discusses and analyzes the theories and applications of the MCDM models used in this study. These MCDMs include those that can be used for objective weighting of the criteria in order to remove the expert bias in the weight assigned to the criteria as well as models that can be used to rank alternatives to select the best alternative. The integrated determination of objective criteria weights (IDOCRIW) is used for objective weightage assignment, while the Combined Compromise Solution (CoCoSo) is used for ranking the alternative.

2.4.1 IDOCRIW weighting model

Zavadskas and Podvezko introduced the IDOCRIW technique in 2016 (Trinkuniene et al., 2017). It is a compensating approach that calculates the comparative effect of loss of characteristics using the entropy and Criterion Impact LOSs (CILOS) techniques and then combines the two approaches for determining the weight of variables. IDOCRIW considers not only the significance of the chosen criteria but also the impact the loss of the chosen criteria can have on establishing the overall criteria weight, resulting in weight values that balance the importance of the criteria with its loss impact to provide more attainable and effective weight values (Vinogradova et al., 2018; Zavadskas et al., 2017). Ayan et al. (2023) provided an in-depth examination of IDOCRIW, while multiple scholars (Alao et al., 2021; Alinezhad and Khalili, 2019) have effectively utilized the IDOCRIW weighting method in a variety of fields of study, including construction and renewable energy, and showed the benefits and drawbacks of IDOCRIW as an objective weighting approach.

The algorithm steps of IDOCRIW are presented as follows:

Entropy weighting steps

Step 1: A decision matrix of the criteria is formed as in **Eq. 8.**

$$X = \left(X_{ij}\right)_{mxn} = \begin{pmatrix} x_{11} & x_{12} & \cdots & x_{1n} \\ x_{21} & x_{22} & \cdots & x_{2n} \\ \vdots & \vdots & \cdots & \vdots \\ x_{1m} & x_{2m} & \cdots & x_{mn} \end{pmatrix}_{m \times n} \tag{8}$$

where; 'X' is the matrix defining the alternatives and the criteria, 'X_{im}' are the possible alternatives, 'X_{jn}' are the evaluation criteria, 'm' is the number of possible alternatives, and 'n' is the number of evaluation criteria.

Step 2: The decision matrix is normalized as in **Eq. 9.**

$$r_{ij} = \frac{x_{ij}}{\sum_{i=1}^{m} x_{ij}} \qquad i = 1, 2\ldots m; j = 1, 2\ldots n \tag{9}$$

Step 3: The degree of entropy is then calculated as in **Eq. 10.**

$$e_j = -\frac{1}{In(m)} \sum_{i=1}^{m} r_{ij}.In\left(r_{ij}\right) \quad 0 \leq e_j \leq 12 \qquad i = 1, 2\ldots m; j = 1, 2\ldots n \tag{10}$$

Step 4: The degree of entropy divergence is gotten as in **Eq. 11.**

$$d_j = 1 - e_j \qquad j = 1, 2 \ldots n \tag{11}$$

Step 5: Entropy weight (w) is then calculated using **Eq. 12**.

$$w_j = \frac{d_j}{\sum_{i=1}^{m} d_j} \tag{12}$$

Note, $\sum_{j=1}^{m} w_j = 1$ j =1, 2 … m.

CILOS weighting steps

As noted by Zavadskas and Podvezko (2016), decision matrix normalization, as in eq. 9, is not a prerequisite in CILOS; normalizing the data helps to see the impact suffered by the criteria.
Step 6: After normalization has been performed, minimized criteria (non-beneficial) values are made beneficial using **eq.13** before the square matrix is produced using eq. 14. However, if all criteria are beneficial, then we skip the step and go to the creation of the square matrix as given in **Eq. 14**.

$$r_{ij} = \frac{\min_{i} r_{ij}}{r_{ij}} \tag{13}$$

$$A = \left\| a_{ij} \right\| \left(a_{ii} = r_{ii}; a_{ij} = r_{kjj} \right) \tag{14}$$

Step 7: The matrix of the relative loss P is then created as given in **Eq. 15** and **Eq. 16.**

$$p = \|p_{ij}\| \tag{15}$$

$$p_{ij} = \frac{r_j - a_{ij}}{r_j} = \frac{a_{ii} - a_{ij}}{a_{ii}} \tag{16}$$

Note: the diagonal elements of the matrix *P* are 0. The elements p_{ij} in the matrix *P* give the relative loss of the *j*th criterion if the *i*th criterion is selected over the best.

Step 8: The matrix F is then determined as shown in **Eq. 17**.

$$F = \begin{bmatrix} -\sum_{i=1}^{m} p_{i1} & p_{12} & \cdots & p_{1m} \\ p_{21} & -\sum_{i=1}^{m} p_{i1} & \cdots & p_{2m} \\ \vdots & \vdots & \cdots & \vdots \\ p_{m1} & p_{m2} & \cdots & -\sum_{i=1}^{m} p_{i1} \end{bmatrix}_{n \times n} \tag{17}$$

Step 9: Then the weights (q_1, q_2 … q_m) of the criteria are obtained by solving the system of homogeneous linear equations given in **Eq. 18**.

$$F \times q_j = 0 \tag{18}$$

Step 10: The criteria weights q_j are the result of the system of the linear equation, which can be solved using the method of Ali et al. (2020). This is shown in **Eq. 19.**

$$q_j = F^{-1} z \tag{19}$$

Where z is a vector near 0, and to determine its value, it is assumed that its first element is closer to 0 while others are zero, and thus vector z (**Eq. 20**) is of the form;

$$Z = [0.000 \;\; 0 \;\; 0 \;\; 0 \;\; 0 \;\; 0 \;\; 0 \;\; 0 \;\; 0 \;\; 0 \;\; 0 \;\; 0 \;\; 0]^T \tag{20}$$

The CILOS weight vector q_j is then normalized so that $\sum_{j=1}^{m} q_j = 1$

IDOCRIW weight step

From the entropy and CILOS weight gotten following each of their algorithm steps, the IDOCRIW weight is then determined through the integration of the entropy and CILOS weight values as given in **Eq. 21**.

$$\omega_j = \frac{w_j . q_j}{\sum_{j=1}^{n} w_j . q_j} \tag{21}$$

It should be noted that the higher the IDOCRIW weight of a criterion, the more significant/important it is.

2.4.2 CoCoSo model

The CoCoSo MCDMs is a relatively new approach that is based on the integration of simple additive weighting (SAW) and the exponentially weighted product model (MEP) for combining compromise perspectives to improve the evaluation of decision-making criteria (Popović, 2021) and was developed by Jazdani et al. (Yazdani et al., 2019a). CoCoSo offers a more balanced and holistic ranking approach since it considers the evaluation of the rank of the alternatives from the perspective of the additive and multiplicative of weights, thereby providing compromise solutions available to the decision maker (Chakraborty et al., 2024). Researchers (e.g., Popovic, 2021) have presented the comprehensive review of the CoCoSo model, while researchers (Ecer et al., 2019; Yazdani and Zaraté et al., 2019; Bui et al., 2023; Do et al., 2022) have successfully applied the CoCoSo model in several disciplines, including the manufacturing sector, the mechanical engineering sector, and the production sector. It should be noted that, prior to the use of CoCoSo for ranking of alternatives, the weights of the criteria must have been calculated using either a subjective weighting model or an objective weightage assignment model.

The algorithm steps of CoCoSo are as follows:

Step 1: The decision matrix has been formed as given in **Eq. 22.**

$$x_{ij} = \begin{bmatrix} x_{11} & x_{12} & \cdots & x_{1n} \\ x_{21} & x_{22} & \cdots & x_{2n} \\ \vdots & \vdots & \cdots & \vdots \\ x_{m1} & x_{m2} & \cdots & x_{mn} \end{bmatrix}_{m\times n} \quad ; \quad i = 1,2\ldots m;\ j = 1,2\ldots n \tag{22}$$

Where; 'X' is the matrix defining the alternatives and the criteria, 'Xim' are the possible alternatives, 'Xjn' are the evaluation criteria, 'm' is the number of possible alternatives, 'n' is the number of evaluation criteria.

Step 2: The normalization of criteria is performed using **Eq. 23** for maximizing and **Eq. 24** for the minimizing criteria.

$$r_{ij} = \frac{x_{ij} - \max\limits_{i} x_{ij}}{\max\limits_{i} x_{ij} - \min\limits_{i} x_{ij}} \tag{23}$$

$$r_{ij} = \frac{\max\limits_{i} x_{ij} - x_{ij}}{\max\limits_{i} x_{ij} - \min\limits_{i} x_{ij}} \tag{24}$$

Step 3: the sum of the weighted comparability sequence (S_i) and the sum of the power weight multiplied by the comparability sequence (P_i) for the alternatives are then calculated accordingly using the Simple Additive Weighting (SAW) and exponentially weighted product model (MEP) approaches as shown in **Eqs. 25** and **26**.

$$S_i = \sum_{j=1}^{n} r_{ij}.w_j \tag{25}$$

$$p_i = \sum_{j=1}^{n} (r_{ij})^{w_j} \tag{26}$$

Note: w_j represents the weight of the criterion *j*, which can be determined using any weightage assignment model.

Step 4: Relative ranks of the alternatives using three aggregation strategies (k_{ia}, $k_{ib,}$ and k_{ic}) are then determined employing **Eqs**. **27, 28,** and **29** respectively.

$$k_{ia} = \frac{s_i + p_i}{\sum_{i=1}^{m} (s_i + p_i)'} \tag{27}$$

$$k_{ib} = \frac{s_i}{\min s_i} + \frac{p_i}{\min p_i'} \tag{28}$$

$$k_{ic} = \frac{\lambda s_i + (1-\lambda) p_i}{\lambda \max\limits_i s_i + (1-\lambda) \max\limits_i p_i} \tag{29}$$

It should be noted that the value of $\lambda = 0.5$ is usually chosen by the decision makers, but the stability of CoCoSo can rely on other values as well (Yazdani and Zaraté et al., 2019).

Step 5: The final ranking of the alternatives (k_i) is then determined using **Eq. 30**. The higher the k_i value, the higher the rank of the alternative.

$$k_i = \frac{1}{3}\left(k_{ia} + k_{ib} + k_{ic}\right) + \left(k_{ia} k_{ib} k_{ic}\right)^{\frac{1}{3}} \tag{30}$$

2.4.3. CRITIC (CRiteria Importance Through Intercriteria Correlation) Model

The CRITIC model (an objective weighting model), a quantitative approach established by Diakoulaki et al. (1995), prioritizes criteria based on their interdependence and statistical significance. The approach works on the concept that how crucial an indicator can be determined by assessing its connection with other criteria as well as the variability it presents. This dual evaluation allows for a more sophisticated understanding of the interactions and impact of criteria in a choice-making framework. The CRITIC technique incorporates variability (std. deviation) and mutual dependence, preventing closely related indicators from controlling the weighting procedure, reducing redundancies, and improving evaluative objectivity. The CRITIC approach's focus on variations and correlation guarantees that every factor offers distinct, unambiguous insights, improving the choice-making system's impartiality and resilience. Conventional techniques may be difficult to adequately depict subtle links among factors in certain instances; however, the CRITIC approach is unique in its capability to effectively handle complex interconnections between variables (Roszkowska, 2013). The CRITIC technique's neutrality in assessing the significance of parameters constitutes one of its noteworthy benefits (Stojanovic et al., 2022; Abdi et al., 2025). The approach improves the dependability of the decision-making process by reducing subjective biases that could arise from expert opinion solely by using statistical measurements of correlation and variability.

By allocating weights based on statistical measurements rather than subjective assessments, the technique makes sure that parameters with higher levels of difference have a bigger impact on the decision-making process and minimizes conceivable prejudices.

The computing processes of the approach are outlined as follows:

Step 1: The decision matrix is formed using **eq. 31.**

$$X = \begin{bmatrix} r_{11} \cdots & r_{1j} \cdots & r_{1n} \\ \vdots \ \ddots & \vdots \ \ddots & \vdots \\ r_{i1} \cdots & r_{ij} \cdots & r_{in} \\ \vdots \ \ddots & \vdots \ \ddots & \vdots \\ r_{m1} \cdots & r_{mj} \cdots & r_{mn} \end{bmatrix}_{m\ x\ n} \quad ;\ i = 1, \cdots, m,\ j = 1, \cdots, n \tag{31}$$

where rij denotes the decision matrix component for the ith preference in the jth variable.

Step 2: Decision Matrix is being normalized according to the maximizing and minimizing (**Eqs. 32a** and **32b**) nature of the criteria

$$\boldsymbol{x_{ij}} = \frac{r_{ij}-r_i^-}{r_i^+-r_i^-} \text{ ; i = 1, …, m, j = 1, …, n, for maximizing criteria} \quad (32a)$$

$$\boldsymbol{x_{ij}} = \frac{r_{ij}-r_i^+}{r_i^+-r_i^-} \text{ ; i = 1, …, m, j = 1, …, n, for minimizing criteria} \quad (33b)$$

where x_{ij} represents a normalised value of the decision matrix for the *i*th alternative in *j*th attribute and $r_i^+ = \max(r_1, r_2, \ldots r_m)$ and $r_i^- = \min(r_1, r_2, \ldots r_m)$

Step 3: The Correlation Coefficient is calculated according to equation

The correlation coefficient among attributes is determined by the **Eq.33**:

$$\boldsymbol{\rho_{jk}} = \sum_{i=1}^{m}(\boldsymbol{x_{ij}} - \bar{\boldsymbol{x}}_j)\,(\boldsymbol{x_{ik}} - \bar{\boldsymbol{x}}_j) / \sqrt{\sum_{i=1}^{m}(\boldsymbol{x_{ij}} - \bar{\boldsymbol{x}}_j)^2 \sum_{i=1}^{m}(\boldsymbol{x_{ik}} - \bar{\boldsymbol{x}}_k)^2} \quad (33)$$

Where $\bar{x}_j$ and $\bar{x}_k$ display the mean of *j*th and *k*th attributes. $\bar{x}_j$ is computed from the equation above. Similarly, it is obtained from $\bar{x}_k$. Also, ρ_{jk} is the correlation coefficient between *j*th and *k*th attributes.

$$\bar{x}_j = \frac{1}{n}\sum_j^n x_{ij} \text{ ; i = 1, …, m}$$

Step 4: The Index C

The standard deviation of each attribute is estimated using the **Eq.34**:

$$\sigma_j = \sqrt{\frac{1}{n-1}}\sum_{j=1}^{n}(x_{ij} - \bar{x}_j)^2; \text{ i = 1, …, m} \quad (34)$$

The index (C) is calculated using the **Eq.35**:

$$C_j = \sigma_j \sum_{k=1}^{n}(1 - \rho_{jk}); \text{ j = 1, ..., n} \quad (35)$$

Step 5: The weight of Attributes

The weight of attributes is determined using the **Eq.36**:

$$w_j = \frac{C_j}{\sum_{j=1}^{n} C_j} \text{ ; j =1, …, n} \quad (36)$$

2.5 The IDOCRIW-CoCoSo Groundwater Potential Index (GPI) Model.

2.5.1 Decision matrix (fishnet points) creation from the thematic layers

To build the GPI, which would be utilized to create the groundwater potential map of the research area, the decision matrix was created by extracting fishnet points (**Table S1**) from all of the GPCFs' thematic maps/layers mentioned in section 2.3. This was accomplished by using the fishnet template map (**Fig. 11**) to extract the pixel values in each of the theme maps by conducting extract values to points in ArcGIS 10.8 software after adding the fishnet template map in turn to the thematic map layers. The conceptual flowchart used in this study to evaluate the groundwater potential of the study region using a variety of objective-based MCDM models is illustrated in **Fig. 12**. Extracted fishnet points of the GPCFs (see supplementary sheet).

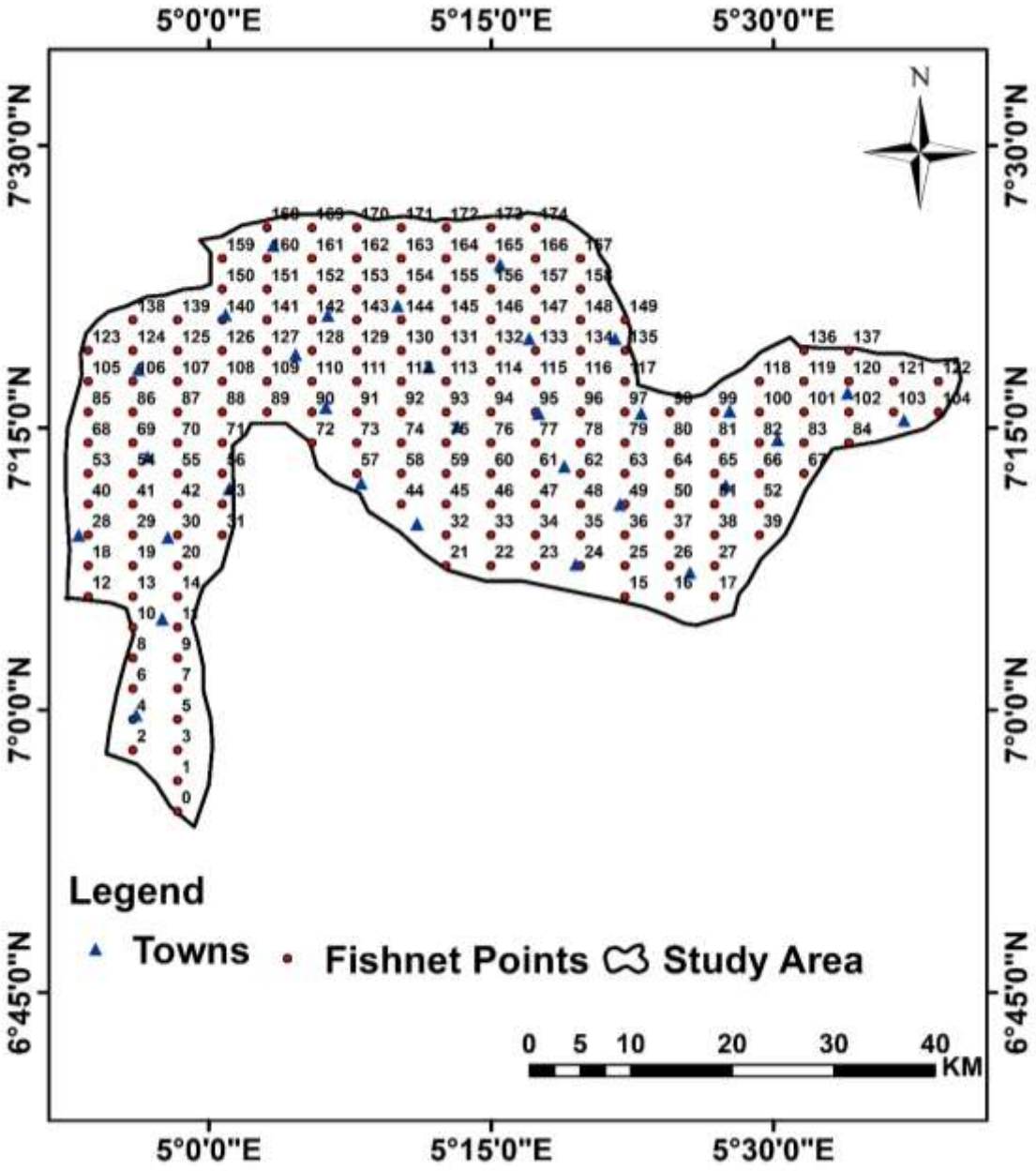

Fig. 11. Fishnet template map of the study area

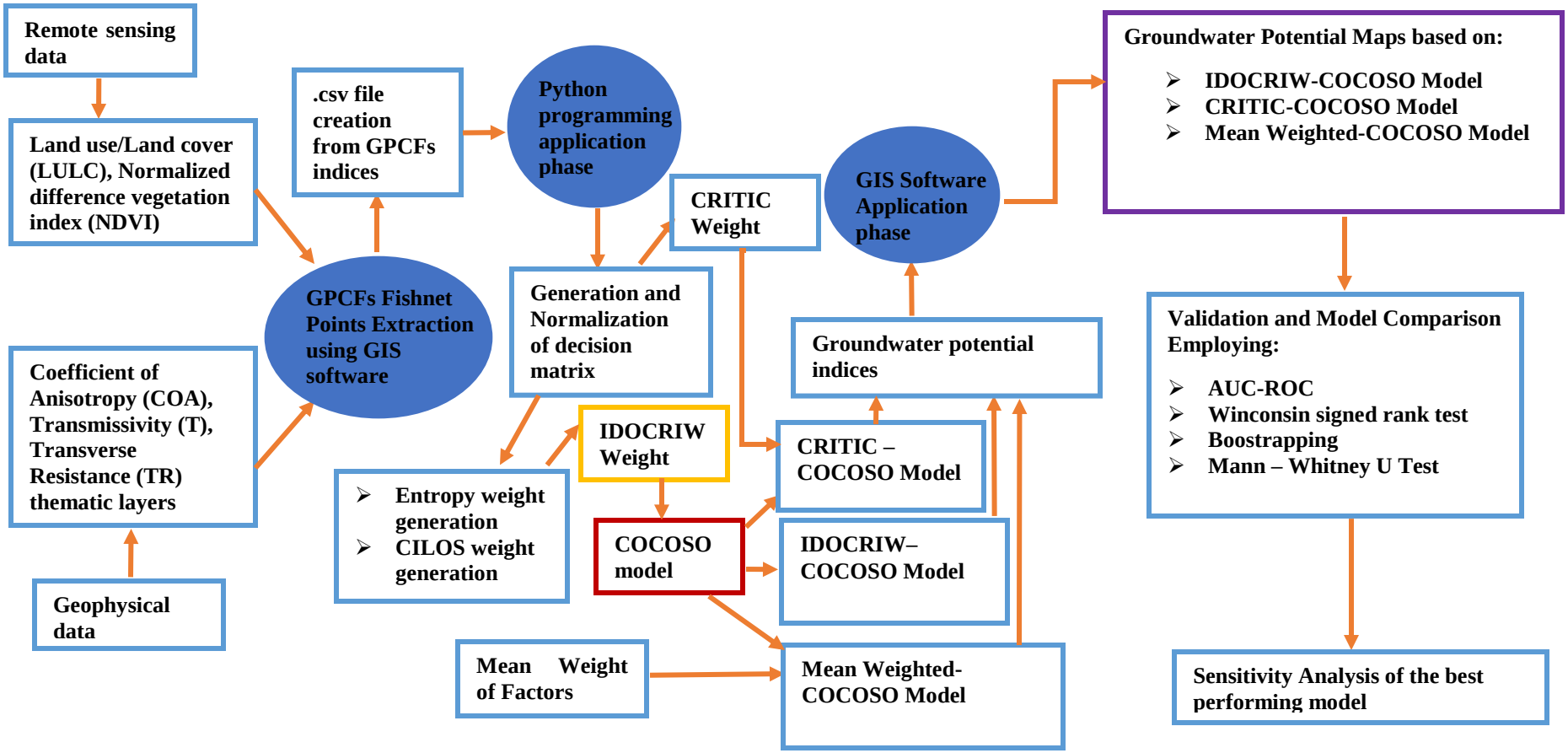

Fig. 12. Flowchart used for establishing the groundwater potential map in the study

2.5.2 Generation of GPI from the IDOCRIW-CoCoSo model

A weighting parameter is required to calculate the weighted comparability sequence (Si) and the sum of the power weight multiplication of the comparability sequence (Pi), as seen in step 3 of the CoCoSo model algorithm. The IDOCRIW–CoCoSo model's concept is that the necessary weighting parameter will be determined through the IDOCRIW weighting algorithm and then entered into the CoCoSo model calculations. As a result, **Eq. 38** provides a possible representation of the GPI generated by integrating the IDOCRIW and CoCoSo models.

$$GPI = P_i \tag{38}$$

where: P_i represents the alternative indices derived through the integration of IDOCRIW weighting and the CoCoSo model, called the IDOCRIW-CoCoSo model, and GPI denotes the groundwater potentiality index. The IDOCRIW-CoCoSo model was used since all computations in the algorithm process were performed using the Python programming language.

2.5.2.1 IDOCRIW weight generation

For constructing the IDOCRIW weights, as given in the computation process laid down in section 2.4.1, the ***initial step*** is to generate the entropy weights. The decision matrix was stored as a comma-separated value (.csv) file format, and leveraging the computation prowess of Python codes, the entropy weights are generated. **Table 3** shows the generated values for entropy, degree of divergence, and the entropy weights for each of the GPCFs.

Table 3. Entropy weight values

GPCFs	Entropy (e_j)	Degree of Divergence (1- e_j)	Entropy weights (w_j)
T	0.944807	0.055193	0.359061
TR	0.918891	0.081109	0.527657
NDVI	0.995575	0.004425	0.028787
LULC	0.991395	0.008605	0.055977
COA	0.995616	0.004384	0.028518

The ***second step*** is to generate the CILOS weights. The choice matrix was stored in comma-separated value (.csv) format and fed into Python code lines to construct the weight system matrix (**Table 4**). The weight system matrix is critical in determining the CILOS weight because it displays the impact loss sustained by each criterion in the major diagonal lines (Zavadskas and Podvezko, 2016). The linear system of **Eq. 39** created by the weight system matrix was then solved using the Ali et al. (2020) technique. The values obtained from the solution of this linear equation serve as the CILOS weights for each of the criteria (**Table 5**).

Table 4. The generated weight system matrix (F)

T (m^2/day)	TR(Ωm)	NDVI	LULC	COA
-2.69779573	0.91624321	0.48692989	0.42857143	0.07060665
0.39504236	-3.72577536	0.40304058	0.50000000	0.05463401
0.88370725	0.94971088	-1.3951657	0.00000000	0.34816245
0.93293066	0.98265288	0.22651209	-0.92857143	0.45463501
0.48611547	0.87716839	0.27868315	0.0000000	-0.92803813

$$\begin{pmatrix} -2.69779557 & 0.91624321 & 0.48692989 & 0.42857143 & 0.07060665 \\ 0.39504236 & -3.72577536 & 0.40304058 & 0.50000000 & 0.05463401 \\ 0.88370725 & 0.94971088 & -1.3951657 & 0.00000000 & 0.34816245 \\ 0.93293066 & 0.98265288 & 0.22651209 & -0.92857143 & 0.45463501 \\ 0.48611547 & 0.87716839 & 0.27868315 & 0.00000000 & -0.92803813 \end{pmatrix} x\, q^T = 0 \quad (39)$$

Table 5. CILOS weight for the criteria

GPCFs	CILOS Weight (q_j)
T	0.105596
TR	0.076461
NDVI	0.204188
LULC	0.306790
COA	0.306966

The *last process* involves generating the IDOCRIW weights by combining the weight values from both the entropy and CILOS weights. To do this, the entropy and CILOS weights from earlier steps were exported into Excel format and then preserved as a .csv file format before being read as input into the Python code lines produced for IDOCRIW weight creation. **Table 6** shows the IDOCRIW weight for each criterion, as well as the entropy and CILOS weight.

Table 6. IDOCRIW weight of the criteria

GPCFs	Entropy weights (w_j)	CILOS weight (q_j)	IDOCRIW weight (ω_j)
T	0.359061	0.105596	0.344479
TR	0.527657	0.076461	0.366555
NDVI	0.028787	0.204188	0.053404
LULC	0.055977	0.306790	0.156027
COA	0.028518	0.306966	0.079535

2.5.2.2 IDOCRIW-CoCoSo generation of the groundwater potential indices (P_i)

The groundwater potential indices (P_i) were generated through the integration of the IDOCRIW weights into the coding process of the CoCoSo algorithm model. In this approach, the GPCFs indices data was read in as a .csv file, and the IDOCRIW weights were created as a numpy array, and using the complete lines of code, the aggregation values (K_{ia}, K_{ib}, and K_{ic}) were generated alongside the final rank (K_i), which served as the groundwater potentiality indices (P_i).

2.6 Generation of GPI from the CRITIC – CoCoSo model

After the initial decision matrix containing the factors at the alternative fishnet points have been normalized based on their minimizing and maximizing direction, following the CRITIC computation steps, the correlation coefficient matrix is generated as given in **Eq. 40.**

$$\begin{pmatrix} 1. & 0.39289045 & -0.08984494 & -0.05387024 & 0.35750972 \\ 0.39289045 & 1. & -0.10549721 & -0.16380167 & 0.33062299 \\ -0.08984494 & -0.10549721 & 1. & 0.31758695 & -0.05803773 \\ -0.05387024 & -0.16380167 & 0.31758695 & 1. & -0.01866801 \\ 0.35750972 & 0.33062299 & -0.05803773 & 0.01866801 & 1. \end{pmatrix} \quad (40)$$

The correlation coefficient was then further analyzed as elaborated in the computation steps of the CRITIC model to generate the CRITIC weight (**Table 7**) of the criteria

Table 7. CRITIC weight of the criteria

GPCFs	**CRITIC weight (q_j)**
T	0.163434
TR	0.098822
NDVI	0.160289
LULC	0.338089
COA	0.239366

The generated CRITIC weight now enters into the weighted comparability sequence (Si) and the sum of the power weight multiplication of the comparability sequence (Pi), of step 3 of the CoCoSo model algorithm. The resulting hybrid model gotten from fusing the computed CRITIC into the algorithm of CoCoSo now forms the CRITIC – CoCoSo model.

2.7 Mean Weighted (MW)–CoCoSo Model

The MW is an uncomplicated and widely applied method for generating objective weight in multi-criteria decision analysis (Singh and Pant, 2021). In this process, equal weight is computed for all the factors leveraging on **eq. 41** and this weight id now being integrated into the computational prowess of CoCoSo as earlier elaborated in the preceding hybrid models.

Criteria weight based on MW = 1/N (41)

N represents the total number of impacting criteria.

All model computations as well as data analysis were done using Python programming language. The Python code lines used in generating the IDOCRIW-CoCoSo GPI is given in the supplementary file.

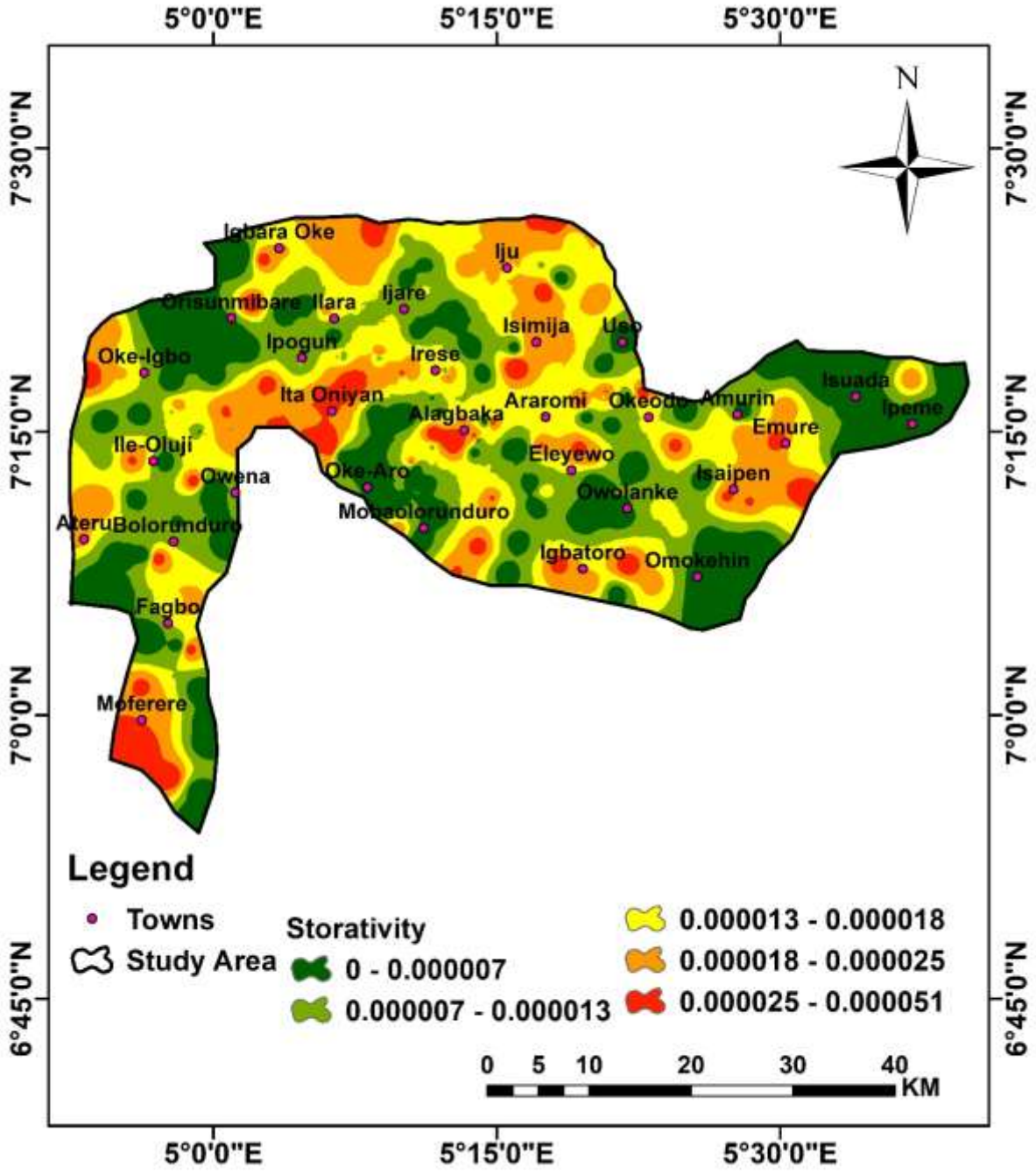

Fig. 13 (a). Storativity map of the study area (b) Pie chart showing the area extent of each of the classes

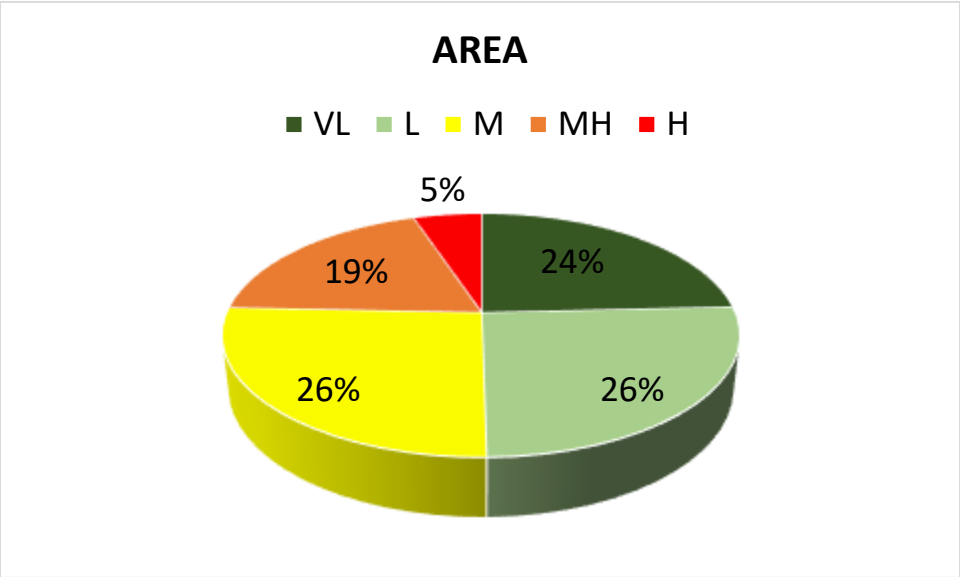

Fig. 13(b). Pie chart showing the area coverage of each S classes

3. Results

3.1 Groundwater potential zoning

Figures 15-18 show the findings of groundwater potential mapping (GPM) with three models in the research region. GPM was divided into five categories: very low (VL), low (L), medium (M), medium-high (MH), and high (H). The geographic patterns of potential for groundwater were consistent across all four models, notably in the very low and high groundwater potential classes (**Table 9**). The research area's western regions have the greatest potential for groundwater resources. The IDOCRIW-CoCoSo model shows that only 10% of the overall catchment region has "high" groundwater potentiality, with an additional 26% classed as "medium high."

According to the CRITIC-CoCoSo statistics, the groundwater potential zone assessments show that the VL, L, M, MH, and H potentials have areas occupied of 5, 18, 25, 36, and 16%, respectively while another 35% has "medium high" potential, according to the mean weighted CoCoSo model. The IDOCRIW-CoCoSo, CRITIC-CoCoSo and MW- CoCoSo models typically display a geographic dimension of 672.12, 970.84 and 821.48 km². This dimension is for the groundwater potential zones falling within the high to medium-high prospect values, respectively (**Table 9**). The geographical disparity displayed in **Figs. 15a–17a** highlights the variations in groundwater potential zone abundance generated by the modelling methodologies whereas **Figs. 15b -17b** showcases the pie chart of the area extent.

Table 9.
Summary of area extent and its percentage coverage for the groundwater potential classes for diverse models used

GWP class	IDOCRIW-CoCoSo (km^2)	IDOCRIW-CoCoSo (%)	CRITIC-CoCoSo (km^2)	CRITIC-CoCoSo (%)	Mean weighted-CoCoSo (km^2)	Mean weighted-CoCoSo (%)
Very low (VL)	112.02	6	93.35	5	74.68	4
Low (L)	485.42	26	336.06	18	298.72	16
Medium (M)	597.44	32	466.75	25	522.76	28
Medium High (MH)	485.42	26	672.12	36	653.45	35
High (M)	186.70	10	298.72	16	317.39	17
Summation	**1867**	**100**	**1867**	**100**	**1867**	**100**

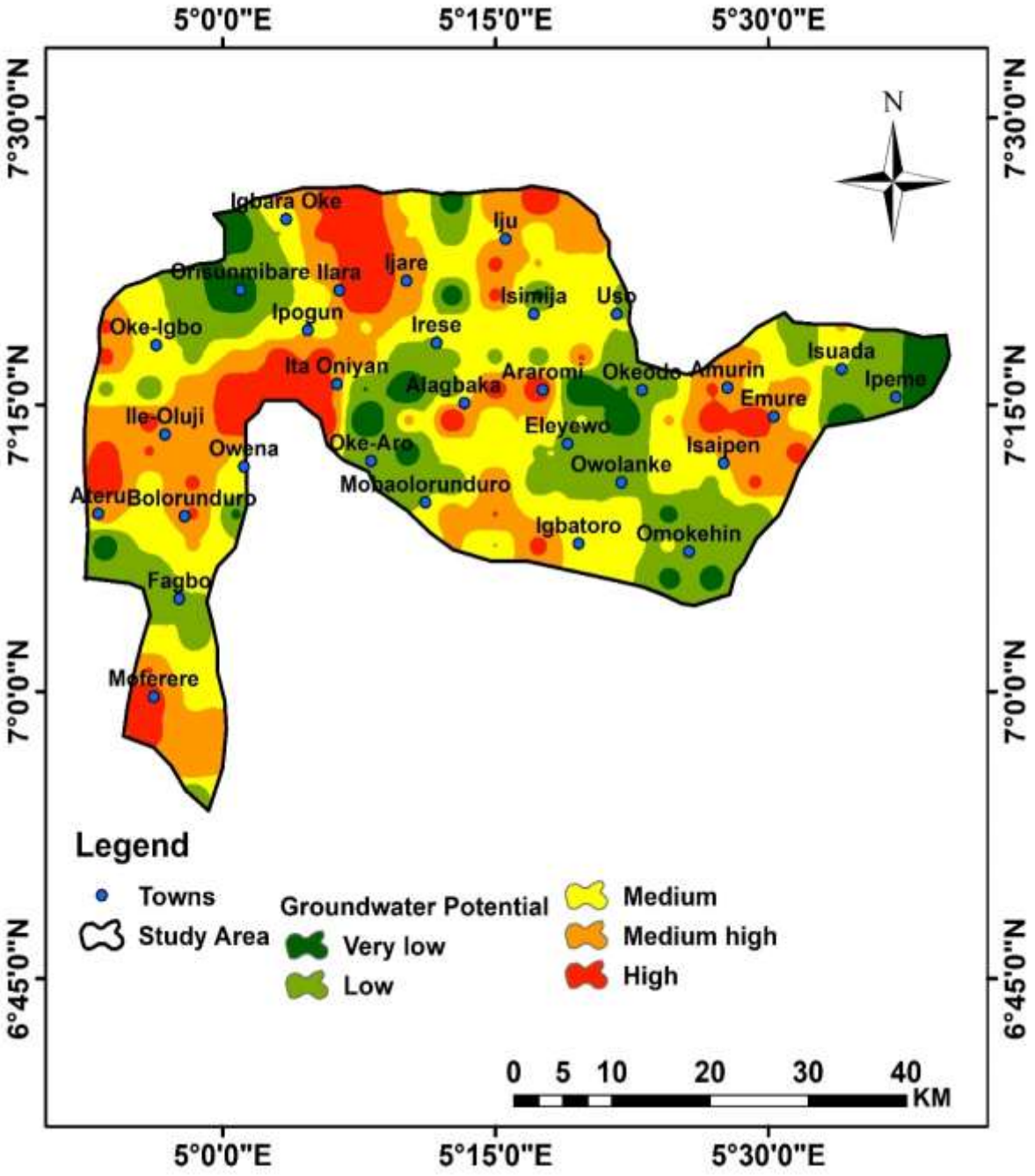

Fig. 15a. The IDOCRIW-CoCoSo groundwater potential map of the study area

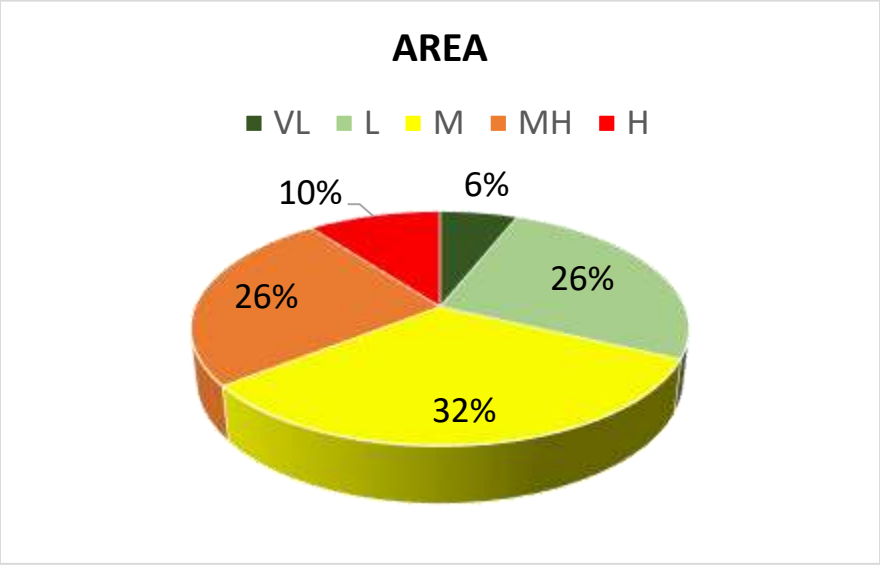

Fig. 15b. Pie chart showing the area coverage of each of the groundwater potentiality classes

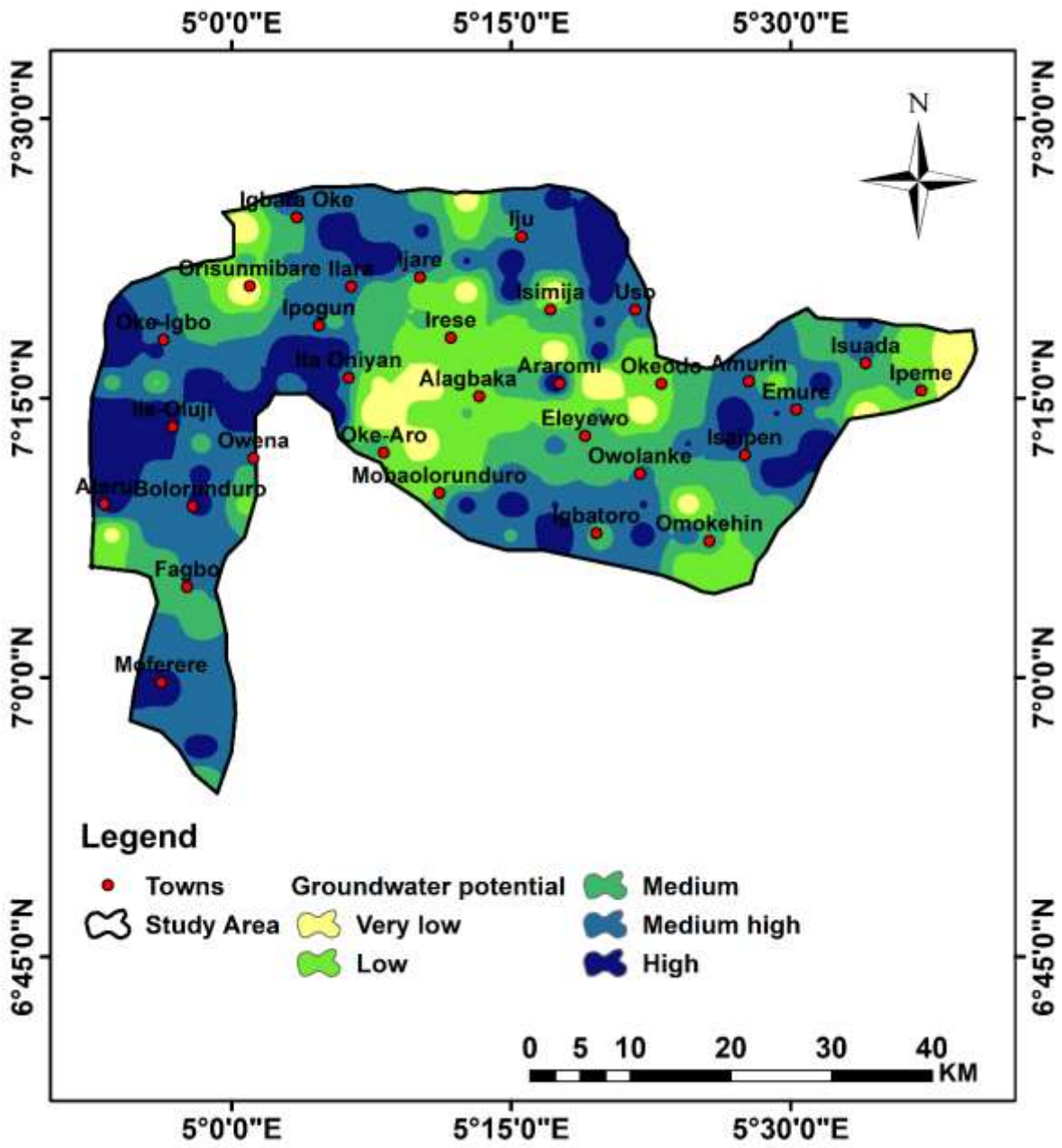

Fig. 16a. Groundwater potential class based on CRITIC-CoCoSo

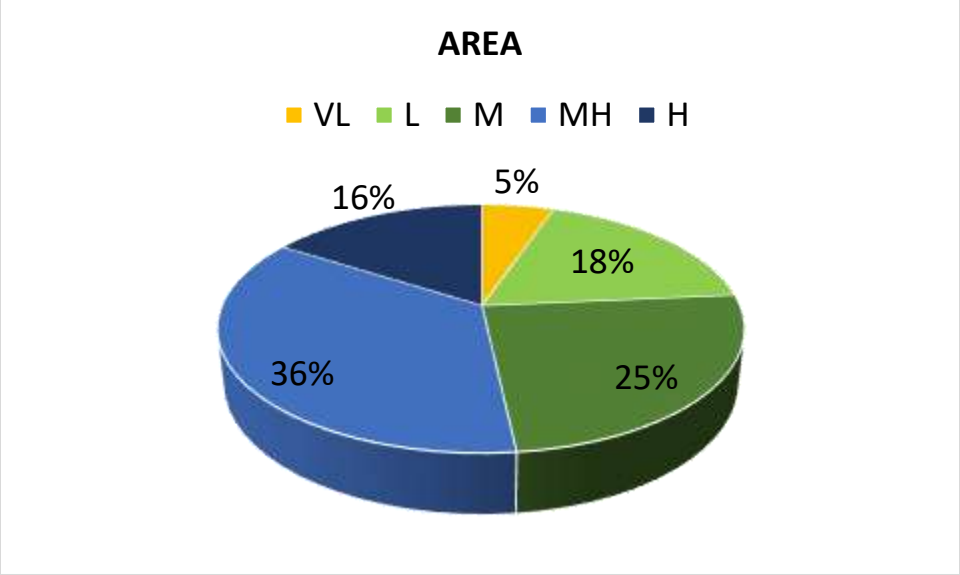

Fig. 16b. Pie Chart of the area coverage of each of the groundwater potential classes

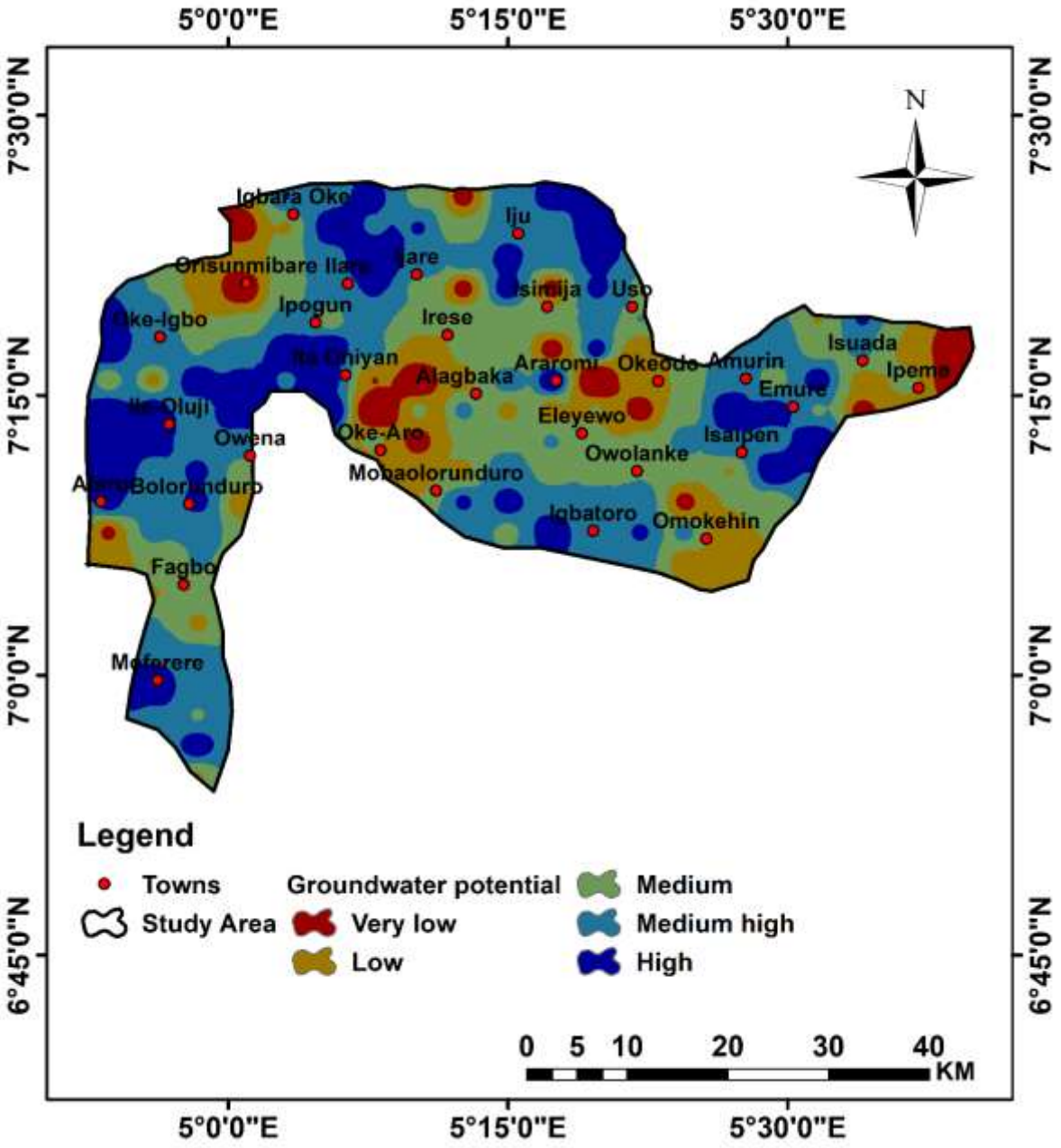

Fig. 17a. The Mean weighted-CoCoSo model groundwater potential map of the study area

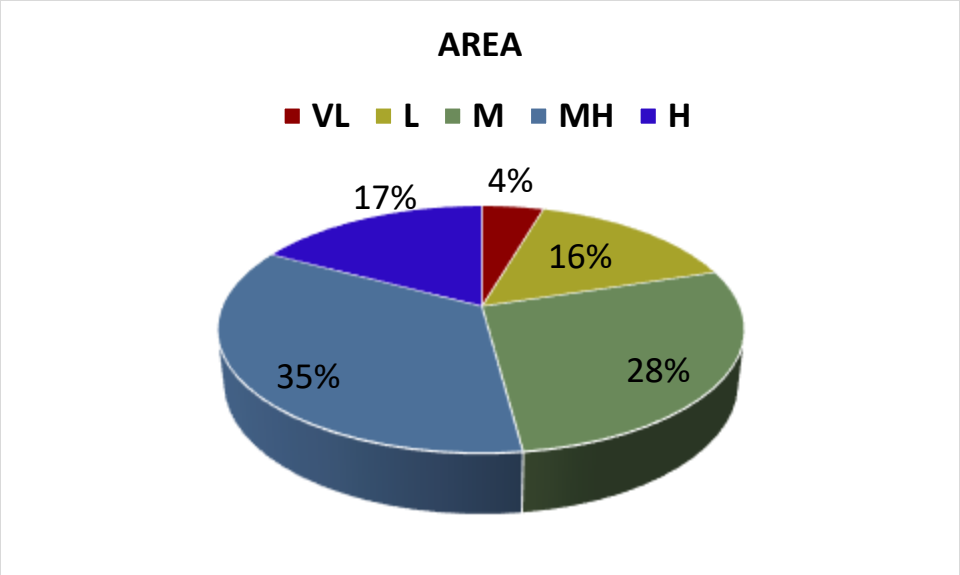

Fig. 17b. Pie chart of the area extent of the groundwater potential classes

3.2 Model Validation Using AUC - ROC Approach

Considering the continuous variability of storativity values and the lack of established categorization standards, unsupervised K-means clustering (k=2) was used to objectively classify low and high groundwater storage zones (Zhu et al., 2021). The generated binary classes were employed as the ground truth, with the GPI index serving as the predictor in a receiver ROC study. The IDOCRIW-CoCoSo had an AUC of 0.83 (**Fig. 17**), indicating that it could statistically distinguish between high and low potential zones. This approach lowers subjectivity and is consistent with current standards of excellence in hydro-model verification using limited labelled data sets. The applied IDOCRIW-CoCoSo groundwater potential evaluation model, with an AUC-ROC of 83%, is considered very good. It is based on the classification of AUC-ROC values into five distinct groups. According to the evaluation conducted by several scholars—Arun Kumar et al. (2021), Masroor et al. (2023), Ali et al. (2023), and Ozegin et al. (2024)—excellent (0.9–1), very good (0.8–0.9), good (0.7–0.8), average (0.6–0.7), and poor (0.5–0.6). The other models' outputs (**Figs. 18-19**) provide the following categories: Mean Weighted-CoCoSo had an AUC of 0.75, ahead of CRITIC-CoCoSo (0.69).

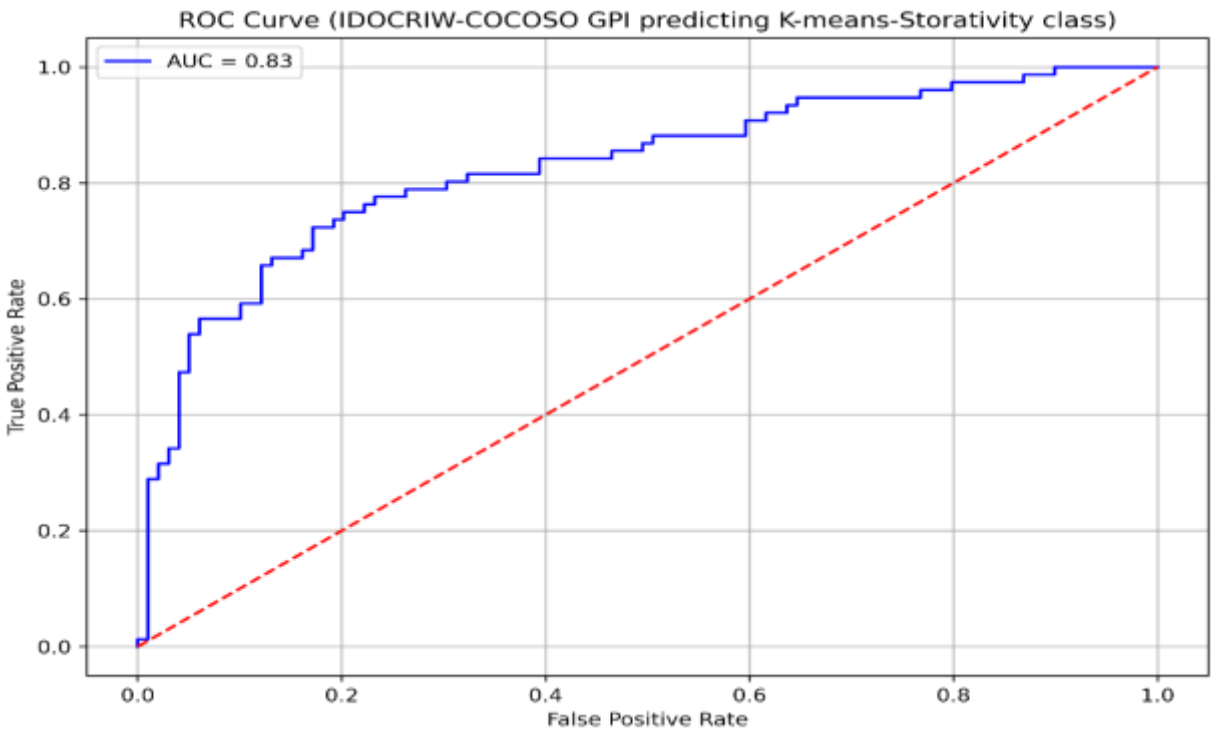

Fig. 17. AUC-ROC accuracy assessment of the python based IDOCRIW-CoCoSo model

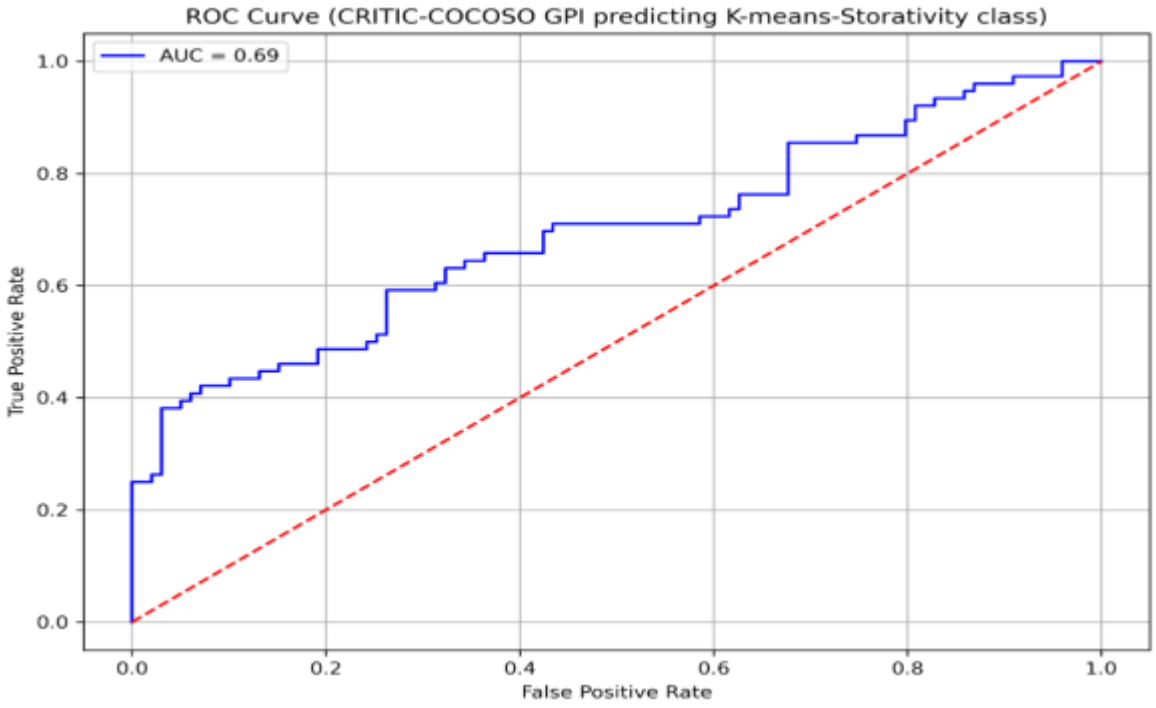

Fig. 18. AUC-ROC accuracy assessment of the CRITIC-CoCoSo model

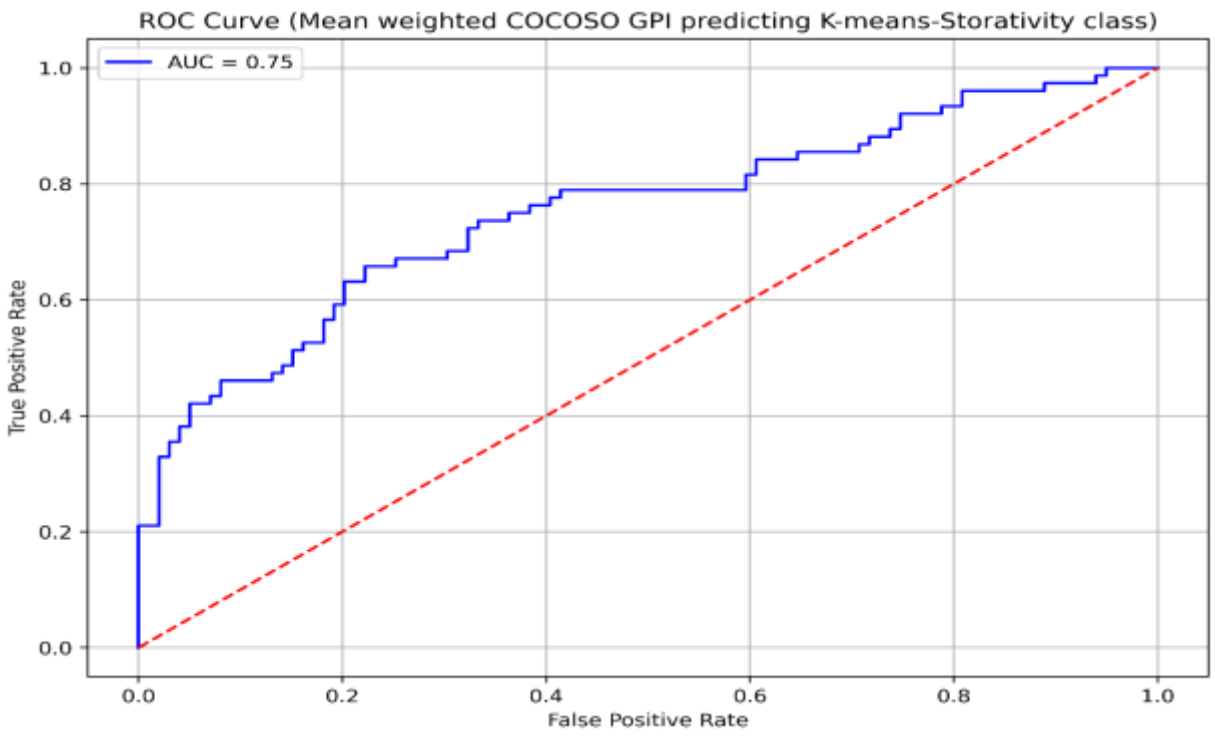

Fig. 19. AUC-ROC accuracy assessment of the Mean Weighted COCOSO GPI model

4. Discussion and computational efficiency of the models

4.1 Discussion of the generated groundwater potential map based on IDOCRIW-CoCoSo model

Assessments of groundwater potential are essential for sustainable water resource management, particularly in areas characterized by diverse geological conditions, where effective groundwater zonation necessitates intricate analysis due to the interplay of multiple possibilities (Gautam et al., 2023). Identifying productive groundwater zones ensures populations have consistent availability to water for household, farming, and industrial use. In this study, a multi-criteria decision-making (MCDM) approach comprising various objective-based modelling algorithms was applied for groundwater potentiality evaluations not only because it was novel in the field but also because it allowed multiple groundwater-influencing variables derived from various data sources to be integrated into the decision-making process. The models' unique attributes include their efficacy in objectively weighting conditioning factors, thus avoiding biases that could arise from expert-based methods, as well as their effortless and efficient management of huge datasets, which contributes to an accurate computational process. In tandem with the study of Chitsaz and Azarnivand (2017), these methodologies are comprehensive, as they utilize multiple thematic layers, including land use/land cover, normalized difference vegetation index, transverse resistance, transmissivity, and coefficient of anisotropy, to develop a thorough evaluation of the groundwater potential of the study area.

The models show the complex connection between the different conditioning factors utilized in the research in the context of the study area's groundwater potentiality assessment. Numerous studies have found that increased groundwater potential is associated with higher plant cover (e.g., Pal et al., 2020; Arunbose et al., 2021; Ozegin and Ilugbo, 2025). A considerable portion of the towns in this study are in the lower groundwater potentiality category, even though the majority of them are in the higher NDVI regions and have higher groundwater potentiality. This finding emphasizes that the total representation of each component in the ultimate objective decision-making is completely determined by its objective weight. The lowest weight allocated to NDVI may have resulted in it having little significance in the final groundwater potential model. Furthermore, lower groundwater potentiality zones will have fewer inhomogeneous strata, implying less weathering, as evidenced by the lower coefficient of anisotropy

found in these areas. Although the majority of the study area falls within the very low to low transverse resistance region (since transverse resistance was given the highest weight), most of these areas fall within the higher groundwater potential region, contrary to expectations that they would fall within the lower groundwater potential regions. This finding indicates that the classification may have been reflected in the very low to low TR regions. The TR value within such very low to low classes may have been sufficient to generate a larger groundwater potential in these areas.

Furthermore, since transmissivity has been analyzed to have a direct relationship with transverse resistance, it was assigned the second highest objective weight, with some of the areas falling within the lower transmissivity regions being distinctively found within the higher groundwater potentiality region. As also found by Khalil et al. (2022), this study thus further indicates that the overall value of a conditioning factor coupled with its higher objective weight is more paramount in determining the influence such a factor will have than the sub-classifications within such a factor. In addition, although LULC was modelled as a minimizing criterion during the algorithm process, some of the built-up area within the study area falls within the higher groundwater potentiality. This may have been as a result of the fact such regions fall within the higher transmissivity and coefficient of anisotropy region, suggesting their higher groundwater potentiality despite being a built-up area. Although geomorphological factors (i.e., rock types, soil types, etc.) were not part of the conditioning factors considered, the adopted geophysical parameters have been recorded to mimic the geological occurrence and thus can be used to infer the hydrologic condition of a region (Omosuyi et al., 2021).

4.2 Computational efficiencies of the models

For ensuring multi-criteria decision-making (MCDM) models produce reliable and reproducible outcomes, it is paramount to assess their computational efficiencies (Pramanik et al., 2021; Sahoo and Goswani, 2023). In this present research, a suite of nonparametric and probabilistic computational efficiency techniques were employed. These techniques help to evaluate the consistency, robustness, and statistical significance of the groundwater potential models. The adopted techniques include the Wilcoxon signed-rank test, Bootstrapped AUC (Area Under the Curve) evaluation and Mann–Whitney U test. The adoption of these tests is guided by the nature of the dataset and the objectives of model performance assessment. Since the groundwater potential indices and the validation data (storativity) are continuous but non-normally distributed, nonparametric approaches offer a more robust means of inference without relying on strict distributional assumptions (Ghosh and Chatterjee, 2022).

4.2.1 Winconxon signed rank test

When the validation data are a proxy (in this case, storativity-derived classes via K-means binarization) instead of specific continuously yielded metrics, t-tests and other parametric methods that assume normality and homoscedasticity become statistically inappropriate. The Wilcoxon signed-rank test was selected alternatively because it is a rank-based, nonparametric technique that is resilient to outliers and does not require that the data be evenly distributed (Ghosh and Chatterjee, 2022). This test is particularly suitable for dependent, paired data sets, enabling a determination of whether the differences in predictions between each alternative model and the reference model (IDOCRIW-CoCoSo) are of statistical significance. The Wilcoxon signed-rank test works effectively for groundwater potential modelling validation settings where the "true" reference is indirect. This is because it concentrates on the ranks of absolute differences rather than raw values, which makes comparisons more accurate when skewed distributions are present. The Wilcoxon signed-rank test, a nonparametric technique appropriate for paired data contrasts, was used to assess the statistical significance of the efficiency variations among the four groundwater potential models. Leveraging the projected GPI values derived from K-means binarization with storativity data (**Table S2**) as the ground-truth reference, this test was utilized to compare the top-performing model (IDOCRIW-CoCoSo) from the other models. Calculating the difference between each set of projections, ranking the absolute differences, and then adding up the ranks independently for both favourable and adverse differences is how the Wilcoxon signed-rank test works. Smaller values of the Wilcoxon statistic, which is the smaller of these two sums, indicate greater dispersion between the models' predictions. The detected differences are evaluated for statistical significance ($p < 0.05$) using a matching p-value (**Table 10**). Table S2. GPI from IDOCRIW-COCOSO with the storativity data (see supplementary sheet).

Table 10. Pairwise Wilcoxon evaluation of the model's AUC values

Model	AUC	Wilcoxon Statistics	p-value	Significant (p<0.05)
IDOCRIW-CoCoSo	0.827352	-	-	-
CRITIC-CoCoSo	0.694444	287	2.31E-28	Yes
Mean Weighted-CoCoSo	0.753456	32	3.13E-30	Yes

4.2.2 Bootsrapping of models' AUC values

The bootstrapping method is a non-parametric resampling approach that estimates a model's capacity variance without making significant assumptions about the fundamental variation in the data (Zhang and Jiang, 2024). In this work, it was used to determine the reliability of the AUC values generated for each groundwater potentiality model. Over 1000 cycles of resampling the dataset with replacements and recalculating AUC values, we generated a distribution of performance metrics for each model (**Fig. 20**). This method is especially useful for datasets with small sample sizes and environmental applications, where the actual distribution of verification information (for example, storativity) is frequently unknown. The computed confidence intervals offer a statistically acceptable range of estimated model performance, which improves the validity of the findings (**Table 11**). IDOCRIW-CoCoSo had the greatest mean AUC (0.851), with a low standard deviation (0.027) and a tight 95% confidence range (0.793–0.899). It demonstrates strong prediction accuracy as well as steady performance throughout repeated samples, emphasizing the model's reliability. CRITIC-CoCoSo exhibited a significantly reduced average AUC (0.701) and more variability (CI: 0.623-0.777), indicating inferior discriminating accuracy and reliability. The MW-CoCoSo model, with a mean AUC of 0.770, performed somewhat well, with larger ranges of confidence than IDOCRIW-CoCoSo, showing a higher sensitivity for sampling variance. The finding that the enhanced efficiency of IDOCRIW–CoCoSo is not random but rather continuously reproducible across all resampling circumstances is supported by the distinct separation of the confidence ranges between IDOCRIW–CoCoSo and the other models.

Table 11. Bootsrapped result

Models	Mean AUC	Std. Dev	95% Confidence Interval (CI) (Lower, Upper)
IDOCRIW-CoCoSo	0.851	0.027	(0.793, 0.899)
CRITIC-CoCoSo	0.701	0.038	(0.623, 0.777)
Mean Weighted-CoCoSo	0.770	0.037	(0.694, 0.839)

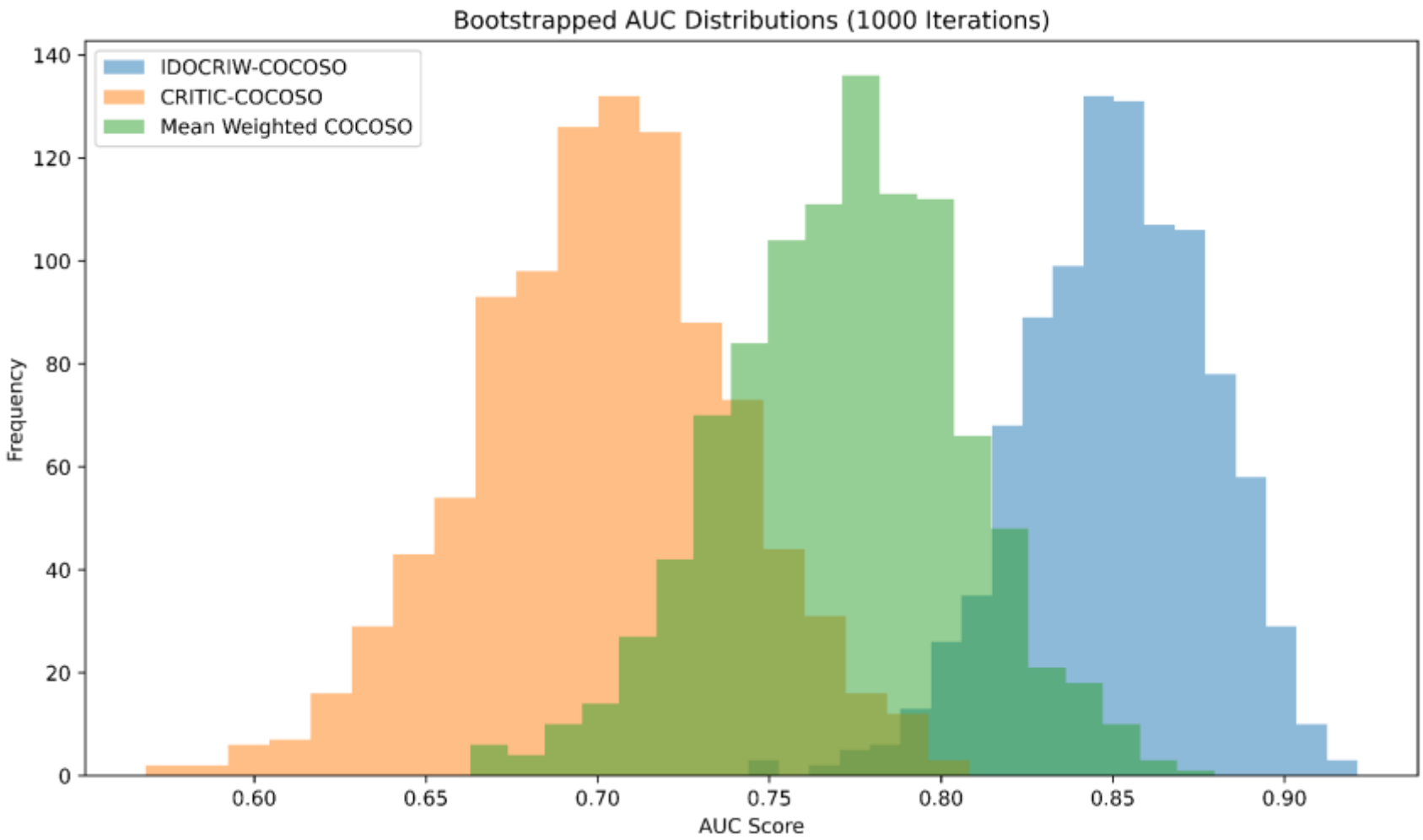

Fig.20. Histogram of the bootstrapped AUC results for the models

4.2.3 Mann-Whitney U Test

The Mann-Whitney U test provides a complementary pairwise comparison between competing models, enabling the identification of the statistically superior model when multiple algorithms are applied to the same spatial domain (Emerson, 2023). The Mann–Whitney U test was used on the bootstrapped AUC distribution to determine if the top-performing model (IDOCRIW-CoCoSo) was better than the other three. This non-parametric rank-based test determines if one model's AUC value distribution is consistently larger than another's. Results that have significance ($p < 0.05$) suggest that random variation is not likely to be the cause of the outcome discrepancy (**Table 12**).

Table 12. Mann-Whitney U Test

Comparison	U-statistic	p-value	Significant ($p < 0.05$)
IDOCRIW–CoCoSo vs CRITIC–CoCoSo	999,510	< 0.000001	Yes
IDOCRIW–CoCoSo vs Mean Weighted–CoCoSo	963,176	< 0.000001	Yes

The results confirm statistically significant differences across all model comparisons, with the IDOCRIW-COCOSO consistently outperforming the other frameworks. The extremely low p-values (< 0.000001) signify that the likelihood of obtaining such differences by random variation is negligible, thereby establishing the IDOCRIW–COCOSO model as the most reliable and effective approach among those tested.

4.2.3 Sensitivity analysis (SA) of the IDOCRIW-CoCoSo model

The SA of the model was carried out by evaluating the reliability of the IDOCRIW-CoCoSo model through the adjustment of the objective weights, as the utilization of the CoCoSo model for ranking intentions is the focus of this study. Nonetheless, a number of studies (Yazdani and Zarate et al., 2019; Rasoanaivo and Zaraté, 2024) have demonstrated the CoCoSo model's stability at λ values that differ from the one used in this study ($\lambda = 0.5$).

To establish the corresponding criterion weights in six scenarios (Scenarios 1–6), the highest weighted factor (TR) value is varied from 25% to 50% in 5% increments (**Table 13**). Each scenario's IDOCRIW-CoCoSo groundwater potential indices (**Table 13**) were generated, and they were then used to create a heatmap (**Fig. 21**). By analyzing the data heterogeneity in every scenario at the fishnet sites, the heat map was created. Even after modifying the most crucial weight to produce six distinct scenarios, the data shows less fluctuation at most of the fishnet points, demonstrating the model's resilience.

Table 13. IDOCRIW Weight of the factors on varying the TR weight by a step of 5% over 6 different instances

Factors	Scenario 1	Scenario 2	Scenario 3	Scenario 0	Scenario 4	Scenario 5	Scenario 6
	TR at 25%	TR at 30%	TR at 35%	Original Value	TR at 40%	TR at 45%	TR at 50%
T	0.407864	0.380673	0.353482	**0.344479**	0.326291	0.299100	0.271909
TR	**0.250000**	**0.300000**	**0.350000**	**0.366555**	**0.400000**	**0.450000**	**0.500000**
NDVI	0.063230	0.059015	0.054800	**0.053404**	0.050584	0.046369	0.042154
LULC	0.184736	0.172420	0.160105	**0.156027**	0.147789	0.135473	0.123157
COA	0.094170	0.087892	0.081614	**0.079535**	0.075336	0.069058	0.062780

SA was also carried out using the variability index (VI) (i.e. the Standard Deveiation) as an indirect indicator to assess the groundwater potential model's reliability under various objective weight situations. A spatial perspective of model variability is provided by the generated heatmap (**Figure 21**), which shows the VI values over several fishnet locations and situations. With the majority of fishnet cells showing values below 1.0, the research shows that the VI diversity over the study area is primarily low to moderate. This implies that even when objective weighting varies, the model has a high level of spatial stability and less variability. This conclusion is further supported by the heatmap's horizontal banding pattern, which shows that most sites behave consistently throughout contexts. Equally, bright yellow bands were used to identify localized zones with high VI values (about 2.5). These areas could correspond to environmentally sensitive or data-scarce regions where model results are more vulnerable to weight perturbations. Such localized sensitivity calls for additional study to guarantee that these regions do not have a disproportionate impact on entire model projections.

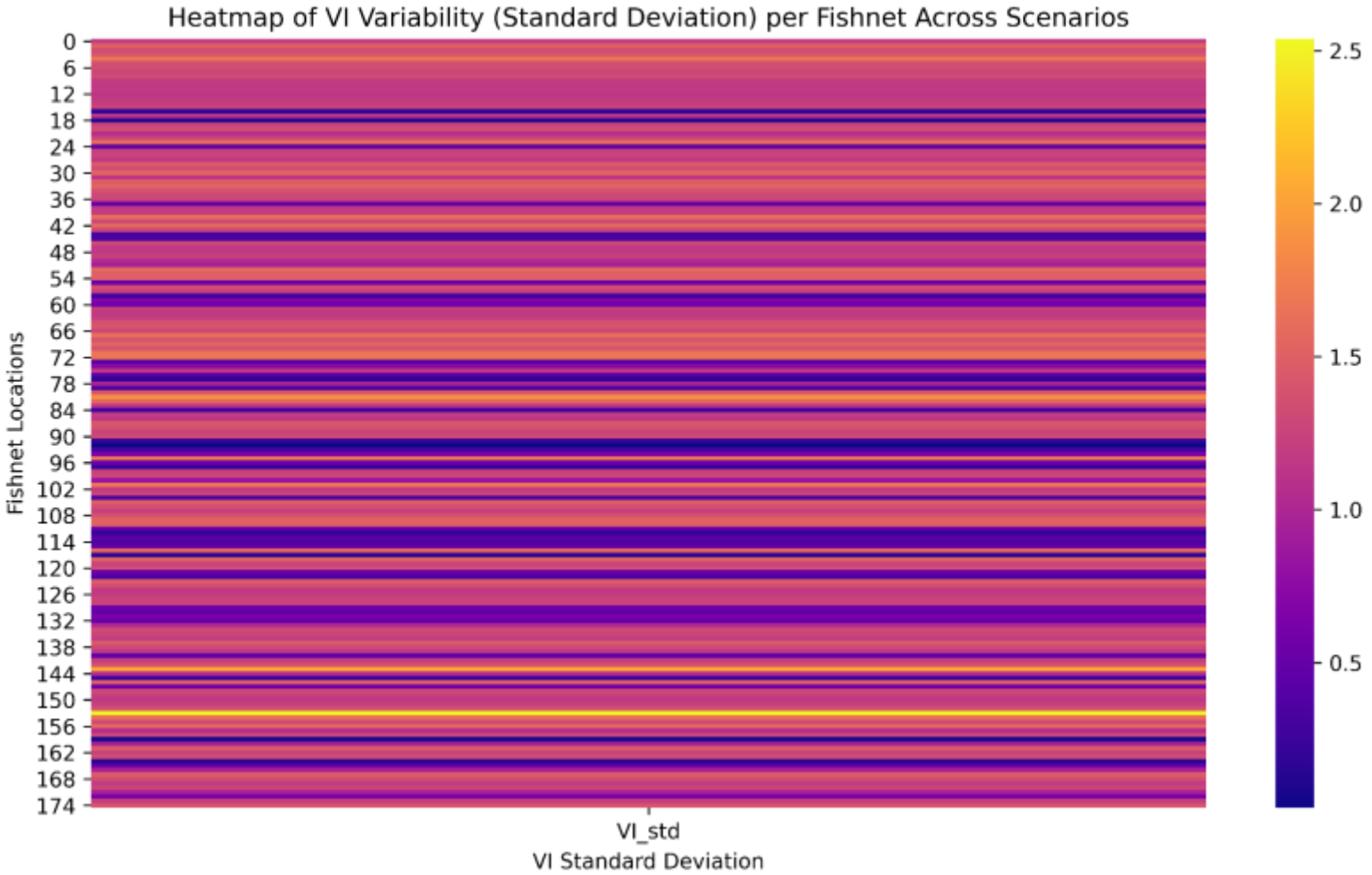

Fig. 21. Heatmap of the sensitivity analysis result

5. The synchronization of the Sustainable Development Goals (SDG)

The study contributes to SDG 6 through the identification of sustainable groundwater (GW) utilization possibilities and methods for minimizing risk for host communities. The mapping of high-potential zones helps to guarantee widespread distribution of access to clean water (Ozegin et al., 2024a). Artificial recharge proposals improve aquifer storage capacity, which supports SDG 6.4 by enhancing the efficiency of water usage and guaranteeing sustainable GW supplies (Ozegin et al., 2024b, c; Carvalho Marques et al., 2025). The artificial replenishment guidelines provide practical alternative strategies for increasing groundwater reservoirs and mitigating the effects of fluctuations in the climate, thereby contributing to climate change adaptation and mitigation efforts. Sustainable extraction solutions help to reduce natural habitat damage while also meeting ecological flow requirements in groundwater-dependent environments. Policy considerations include incorporating spatial recharge potential data into water resource management and regulatory frameworks.

6. Conclusion

The objective-based models used in this study—IDOCRIW-CoCoSo, CRITIC-CoCoSo and MW-CoCoSo—have been demonstrated to be significant for evaluating groundwater potentiality in a complex geologic region. This was accomplished by combining important geophysical and remote sensing metrics, such as transmissivity, coefficient of anisotropy, land use/land cover, normalized difference vegetation index, and transverse resistance. Despite the adjustments required to solve challenges associated with water scarcity and climate variability, the methodology used in this study—which is systematic in nature and based on conceptual requirements—can be employed anywhere data is available. The GW recharge potential map serves as a repository for resource knowledge that may be updated on a regular basis by adding fresh data and other kinds of themed maps. The study demonstrates how combining remotely monitored features, groundwater well data, and geophysical data can result in a dependable mapping of groundwater possibilities. These can be efficiently employed in the decision-making process to focus on specific production areas rather than drilling in incorrect locations or expensively extending existing wells. The use of management strategies is expected to improve groundwater recharge naturally, expanding the amount of water available to the local population. The findings demonstrate how well the objective-based models reflect the complex interactions between various hydrogeological elements, offering a solid foundation for managing groundwater resources. The validation findings substantially improve the confidence of the methods used. This structure will be beneficial for quickly evaluating groundwater recharge and directing the positioning of artificial recharging systems and other watershed governance projects. Notwithstanding intensive and systematic evaluations, this work has some limitations. The success of the eventual groundwater potential assessment determined by the chosen approach may have been diminished if geological and climatic variables had not been taken into account, as the current study primarily relies on the quality and availability of the input data. Additionally, the validation was undertaken using the sparse borehole yield data, which could not have mirrored the actual case if the data had been disseminated throughout the entire study. Therefore, it is suggested that many factors from both geomorphological and climatic data be incorporated into the development of groundwater models in order to increase the accuracy and reliability of the model.

However, given the IDOCRIW-CoCoSo model's performance accuracy, it represents a promising approach to groundwater potentiality evaluations, strengthening decision-making processes for sustainable water resource planning in not only a complex geological environment but also a validation data-scarce setting. The methodology proposed in this study can thus be used by scholars working in a similar data-scarce, multifaceted geologic setting, and the results are also reliable and applicable to important stakeholders in the groundwater domain.

Appendix

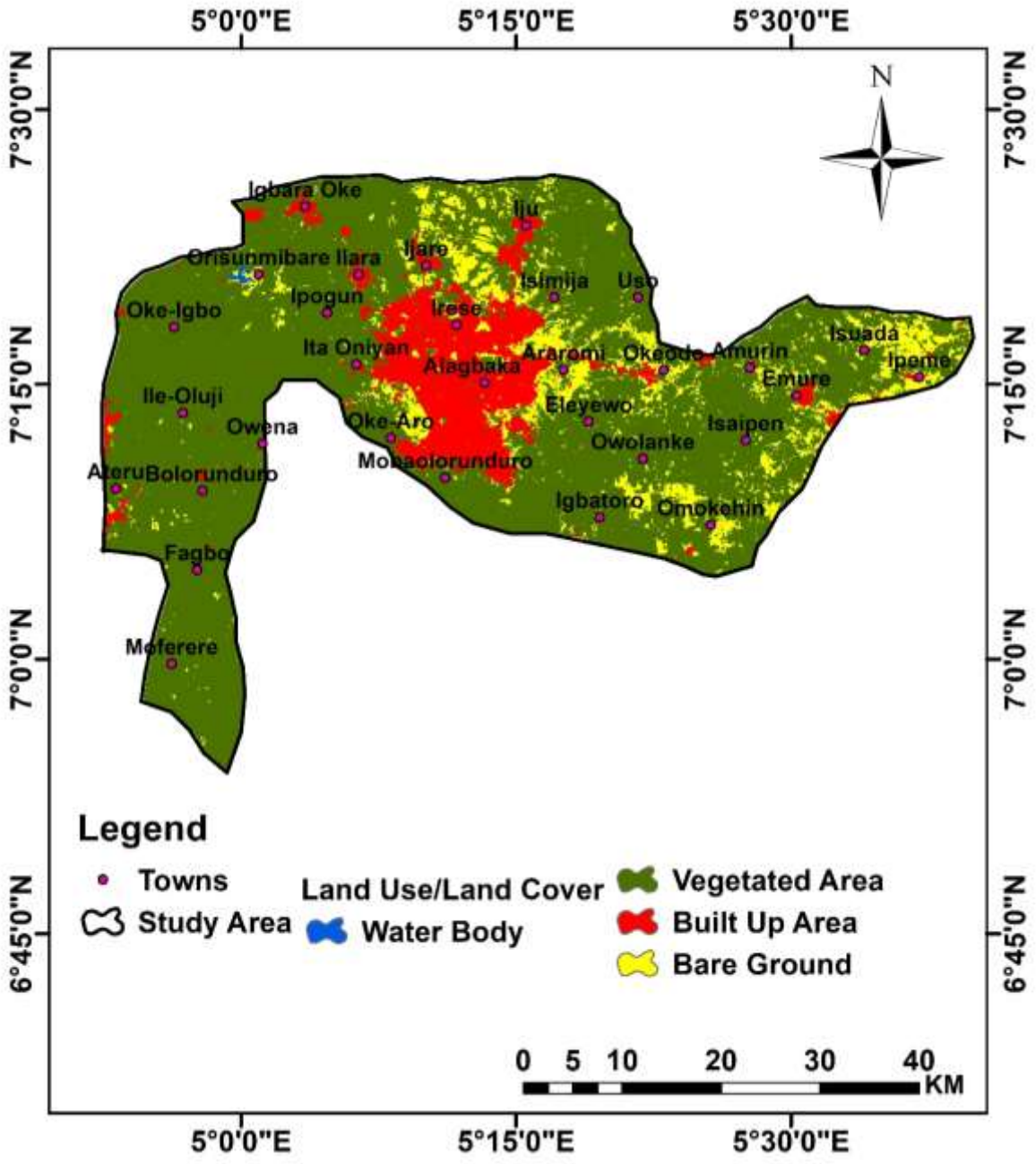

Fig. 6(a): LULC thematic map of the study area

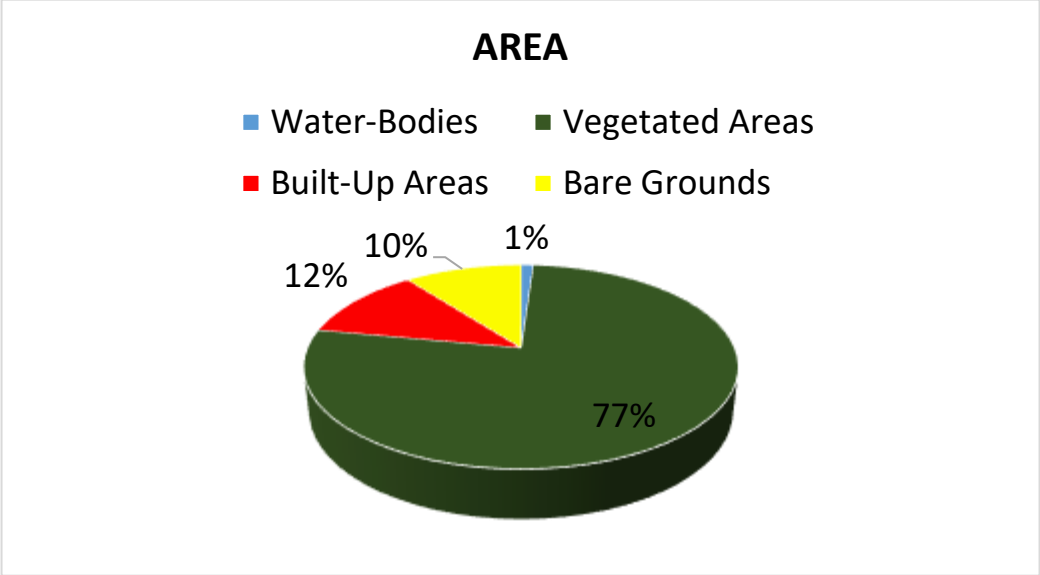

Fig. 6(b): Pie chart showing area coverage of each of the LULC classes

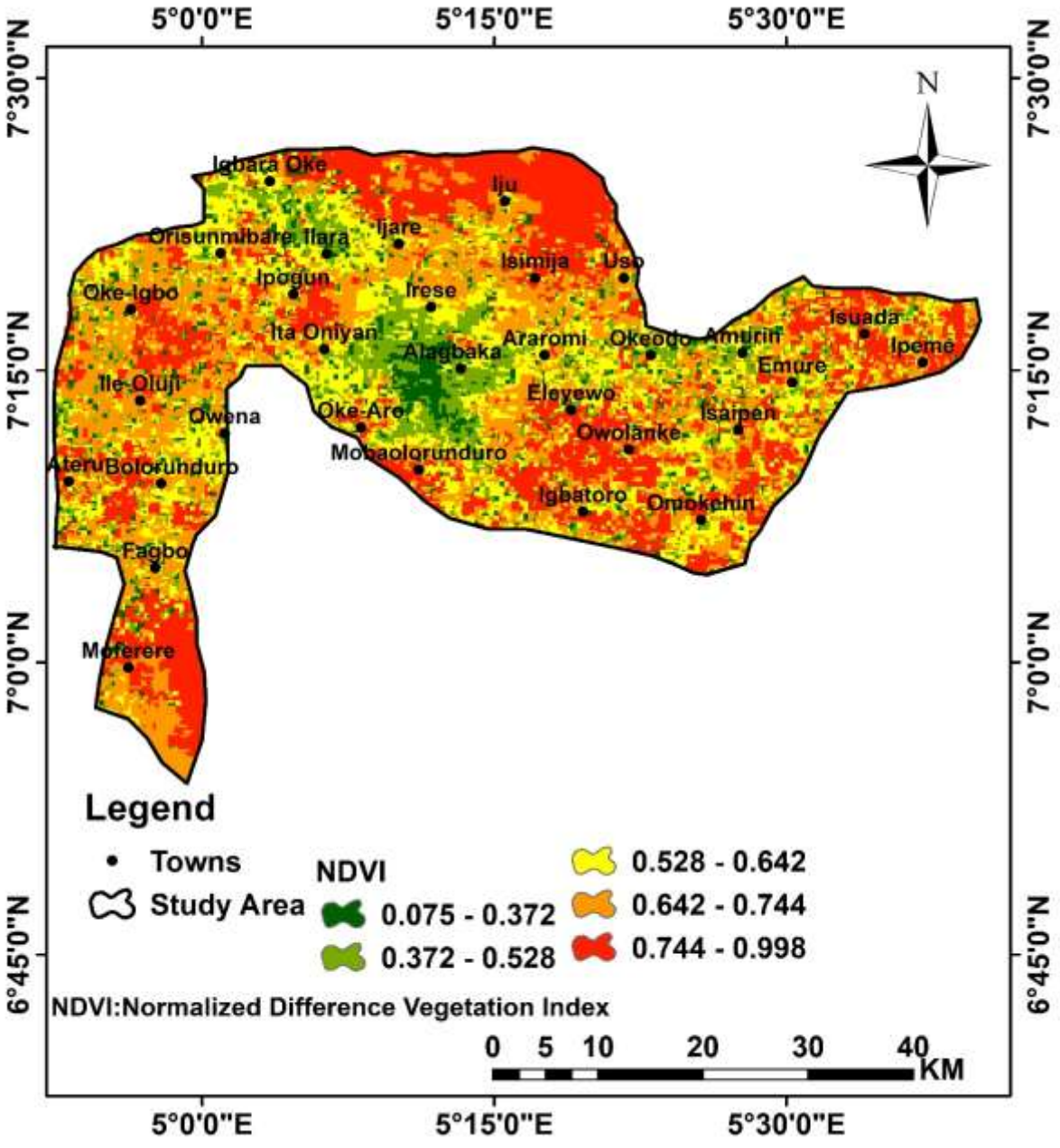

Fig. 7(a): NDVI thematic map of the study area

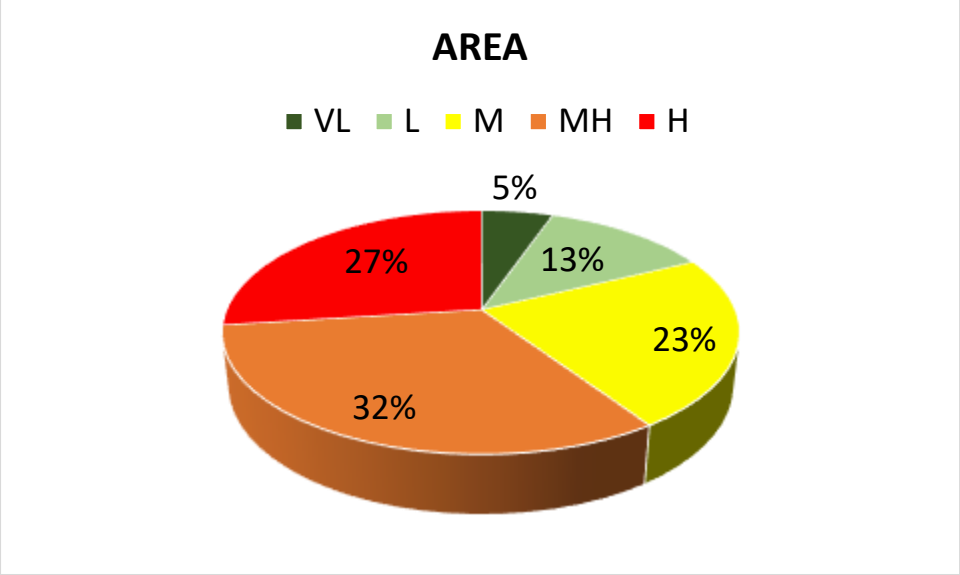

Fig. 7(b): Pie chart showing area coverage of each NDVI class

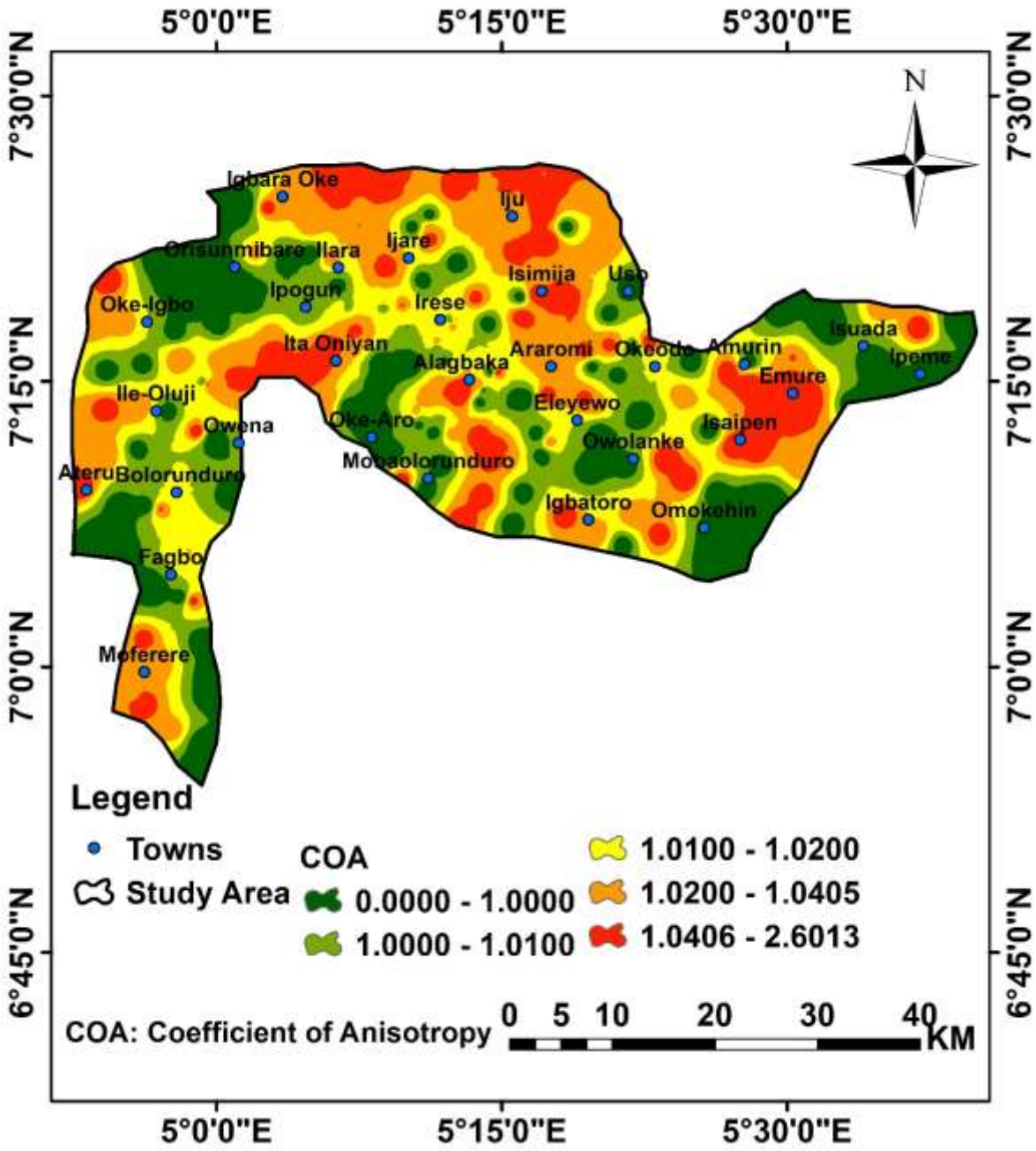

Fig. 8(a): COA thematic map of the study area

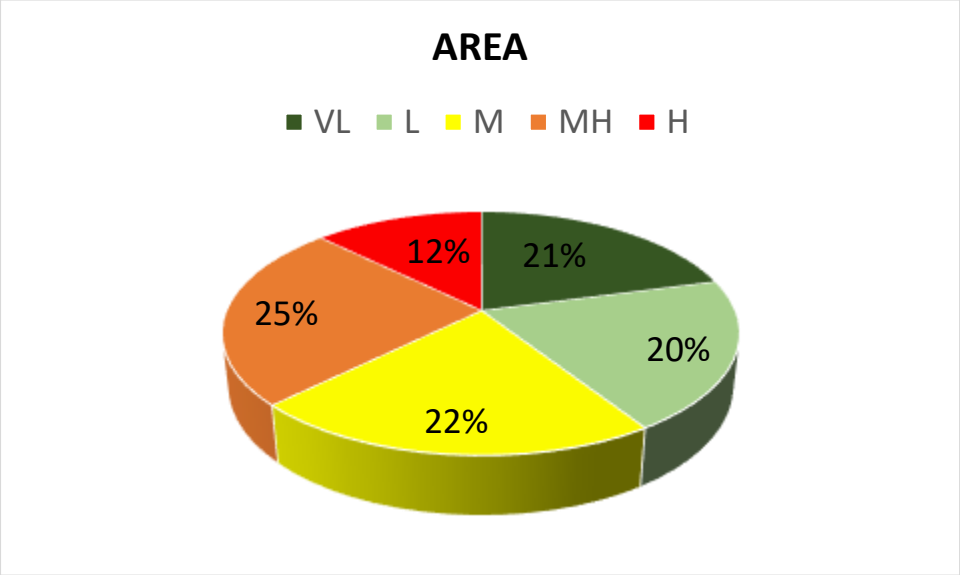

Fig. 8(b): Pie chart showing area coverage of each COA class

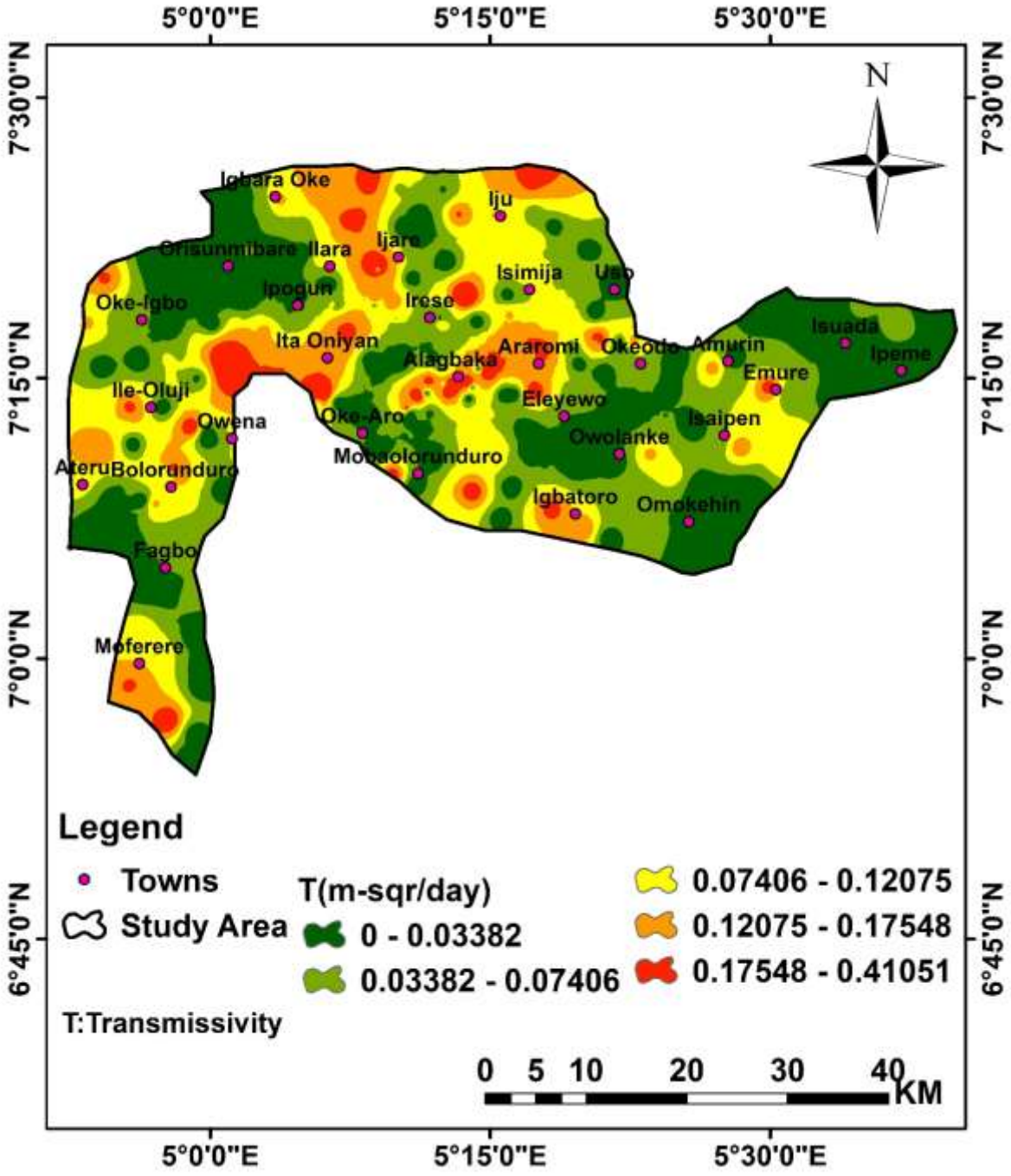

Fig. 9(a): T thematic map of the study area

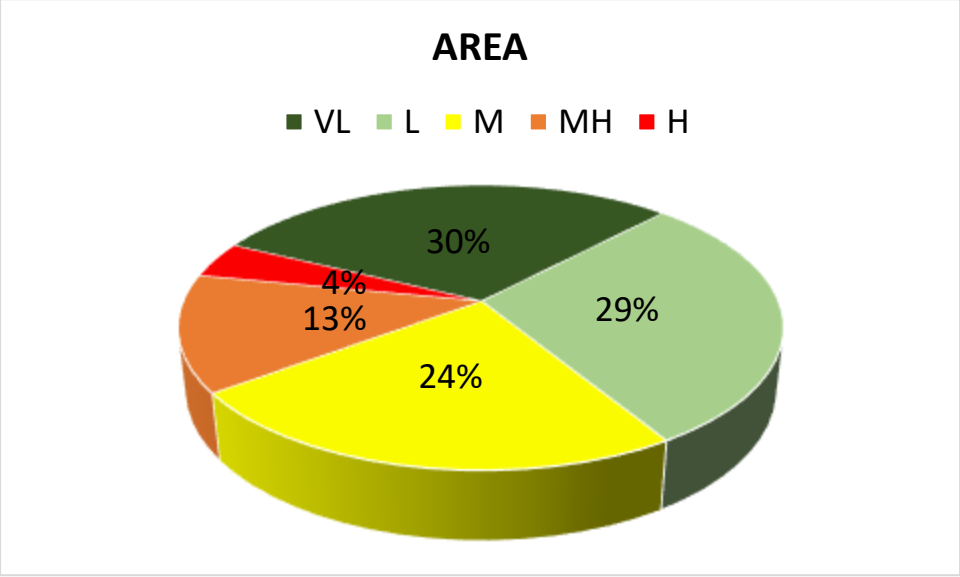

Fig. 9(b): Pie chart showing area coverage of each T classes

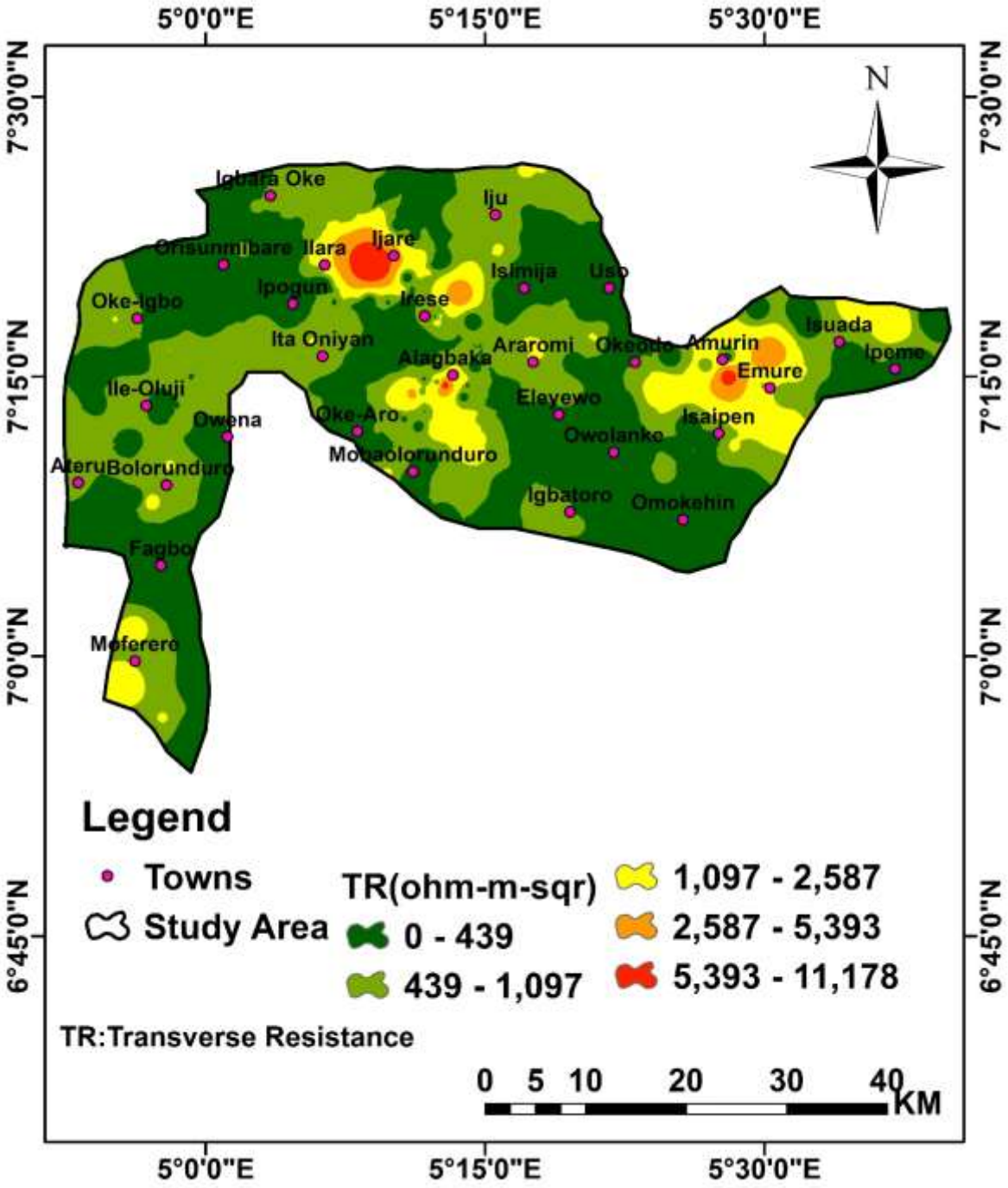

Fig. 10(a): TR thematic map of the study area

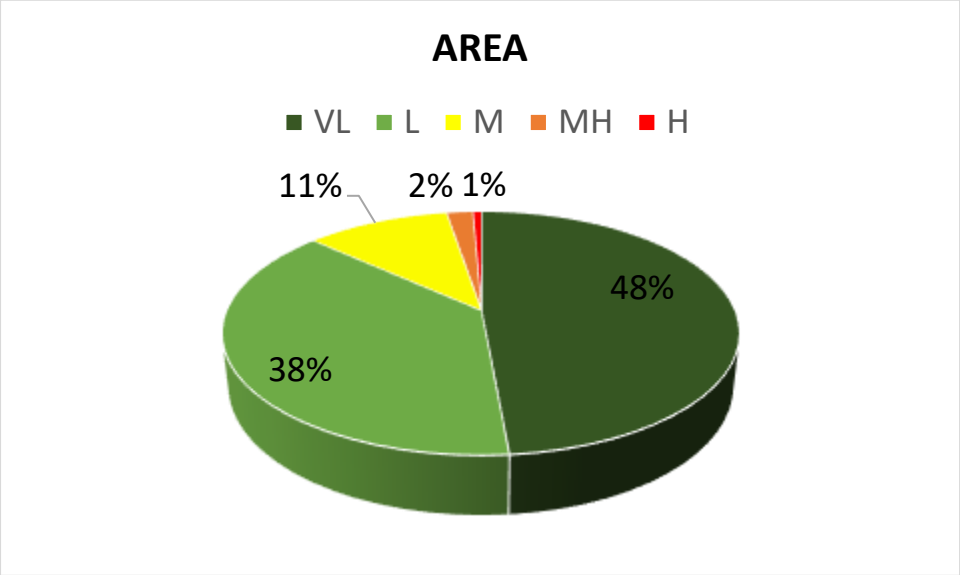

Fig. 10(b). Pie chart showing the area coverage of each TR classes

References

Abdi, A.P., Damci, A., Turkoglu, H., Kirca, V.S.O., Demirkesen, S., Sadikoglu, E., Arslan, A.E., 2025. A Geographic Information System-Based Integrated Multi-Criteria Decision-Support System for the Selection of Wind Farm Sites: The Case of Djibouti. Sustainability 17, 2555. https://doi.org/10.3390/su17062555.

Abebrese, S., Anornu, G.K., Kabo-Bah, A.T., Dekongmen, B. W., Sunkari, E. D., 2022. Assessment of groundwater potential zones using GIS and remote sensing techniques in the Bole District, Savannah Region, Ghana. International Journal of Energy and Water Resources 6(4), 445-456.

Abuzied, S.M., Alrefaee, H.A., 2017. Mapping of groundwater prospective zones integrating remote sensing, geographic information systems and geophysical techniques in El-Qaà Plain area, Egypt. Hydrogeology Journal 25(7), 2067.

Adeoti, B., Okonkwo, C.T., 2016. Structural geology of the basement complex rocks in Iwaraja Area, Southwestern Nigeria. International Letters of Natural Sciences 58, 16-28.

Adeyemo, A.A., Adeoye, I.O., Bello, O.S. 2017. Adsorption of dyes using different types of clay: a review. Applied Water Science 7, 543-568.

Adiat, K.A.N., Kolawole, A.O., Adeyemo, I.A., Akinlalu, A.A., Afolabi, D.O., 2024. Assessment of groundwater resources from geophysical and remote sensing data in a basement complex environment using fuzzy-topsis algorithm. Results in Earth Sciences 2, 100034.

Ajayi, O.G., Nwadialor, I.J., Odumosu, J.O., 2022. Assessment and delineation of groundwater potential zones using integrated geospatial techniques and analytic hierarchy process. Appl Water Sci 12, 276 https://doi.org/10.1007/s13201-022-01802-4

Akinlalu, A.A., Adegbuyiro, A., Adiat, K.A.N., Akeredolu, B. E., Lateef, W.Y., 2017. Application of multi-criteria decision analysis in prediction of groundwater resources potential: a case of Oke-Ana, Ilesa Area Southwestern, Nigeria. NRIAG Journal of Astronomy and Geophysics 6(1), 184-200.

Akinlalu, A.A, Adebayo, O.S., Afolabi, D.O. 2022 Groundwater Potential Mapping Using Geophysical Data and Entropy Method in a Typical Basement Complex Environment, Southwestern Nigeria. Trop. J. of Eng., Sci. and Techn. 1(1),14-50

Akinluyi, F.O., Olorunfemi, M.O., Bayowa, O.G., 2018. Investigation of the influence of lineaments, lineament intersections and geology on groundwater yield in the basement complex terrain of Ondo State, Southwestern Nigeria. Applied water science 8, pp.1-13.

Akintorinwa, O.J., Atitebi, M.O., Akinlalu, A.A., 2020. Hydrogeophysical and aquifer vulnerability zonation of a typical basement complex terrain: A case study of Odode Idanre southwestern Nigeria. Heliyon, 6(8).

Akinwumiju, A.S., Olorunfemi, M.O., 2019. Development of a conceptual groundwater model for a complex basement aquifer system: The case OF OSUN drainage basin in southwestern Nigeria. Journal of African Earth Sciences 159, 103574.

Al-Abadi, A.M., 2017. The application of Dempster–Shafer theory of evidence for assessing groundwater vulnerability at Galal Badra basin, Wasit governorate, east of Iraq. Applied Water Science 7(4), 1725-1740.

Alao, M.A., Popoola, O.M., Ayodele, T.R., 2021. Selection of waste-to-energy technology for distributed generation using IDOCRIW-Weighted TOPSIS method: A case study of the City of Johannesburg, South Africa. Renewable Energy 178, 162-183.

Ali, R., Sajjad, H., Saha, T.K., Roshani, Masroor, M., Rahaman, M.H., 2023. Effectiveness of machine learning ensemble models in assessing groundwater potential in Lidder watershed, India. Acta Geophys. 72, 2843–2856. https://doi.org/10.1007/s11600-023-01237-8.

Ali, T., Chiu, Y.R., Aghaloo, K., Nahian, A.J., Ma, H., 2020. Prioritizing the existing power generation technologies in Bangladesh's clean energy scheme using a hybrid multi-criteria decision-making model. Journal of Cleaner Production 267, 121901.

Alinezhad, A., Khalili, J., 2019. IDOCRIW Method. In: New Methods and Applications in Multiple Attribute Decision Making (MADM). International Series in Operations Research & Management Science, 277, 133–141. Springer, Cham. https://doi.org/10.1007/978-3-030-15009-9_19.

Aneela M, Kamran A, Abdul Ghani S, Muhammad Afzal J, Babar N and Arshad (2020). Estimation of groundwater potential using GIS modeling in Kohistan region Jamshoro district, Southern Indus basin, Sindh, Pakistan (a case study), Acta Geophysica 68, 155–165. https://doi.org/10.1007/s11600-019-00382-3.

Aouragh, M.H., Essahlaoui, A., El Ouali, A., El Hmaidi, A., Kamel, S., 2017. Groundwater potential of Middle Atlas plateaus, Morocco, using fuzzy logic approach, GIS and remote sensing. Geomatics, Natural Hazards and Risk, 8(2), 194-206.

Arabameri, A., Lee, S., Tiefenbacher, J.P., Ngo, P. T.T., 2020. Novel ensemble of MCDM-artificial intelligence techniques for groundwater-potential mapping in arid and semi-arid regions (Iran). Remote Sensing, 12(3), 490.

Arunbose, S., Srinivas, Y., Rajkumar, S., Nair, N.C., Kaliraj, S. 2021. Remote sensing, GIS and AHP techniques-based investigation of groundwater potential zones in the Karumeniyar river basin, Tamil Nadu, southern India. Groundwater for Sustainable Development 14, 100586.

Ayan, B., Abacıoğlu, S., Basilio, M.P., 2023. A comprehensive review of the novel weighting methods for multi-criteria decision-making. Information 14(5), 285. https://doi.org/10.3390/info14050285.

Ayejoto, D.A., Egbueri, J.C., Agbasi, J.C., Omeka, M.E., Unigwe, C.O., Nwazelibe, V. E., ... Pande, C. B., 2023. Influence of Seasonal Changes on the Quality of Water Resources in Southwestern Nigeria: A Review. Climate Change Impacts on Nigeria: Environment and Sustainable Development 423-447.

Barrett, C.B., Benton, T.G., Fanzo, J., Herrero, M.T., Nelson, R., Bageant, E., Wood, S.A., 2022. Socio-technical innovation bundles for agri-food systems transformation. In: Socio-Technical Innovation Bundles for Agri-Food Systems Transformation. Sustainable Development Goals Series. Palgrave Macmillan, Cham. https://doi.org/10.1007/978-3-030-88802-2_1.

Benjmel, K., Amraoui, F., Aydda, A., Tahiri, A., Yousif, M., Pradhan, B., Abioui, M., 2022. A multidisciplinary approach for groundwater potential mapping in a fractured semi-arid terrain (Kerdous Inlier, Western Anti-Atlas, Morocco). Wate 14(10), 1553.

Bhaskar, A.S., Khan, A., 2022. Comparative analysis of hybrid MCDM methods in material selection for dental applications. Expert Systems with Applications, 209, 118268.

Bhunia, G.S., 2020. An approach to demarcate groundwater recharge potential zone using geospatial technology. Applied Water Science 10(6), 1-12.

Carvalho Marques, M. de, Mohamed, A. A., Feitosa, P., 2025. Sustainable development goal 6 monitoring through statistical machine learning – Random Forest method. Cleaner Production Letters 8, 100088. https://doi.org/10.1016/J.CLPL.2024.100088.

Das, S., Pardeshi, S.D., 2018. Integration of different influencing factors in GIS to delineate groundwater potential areas using IF and FR techniques: a study of Pravara basin, Maharashtra, India. Applied Water Science 8(7), 197.

Dey, S., Shukla, U.K., Mehrishi, P., Mall, R.K., 2021. Appraisal of groundwater potentiality of multilayer alluvial aquifers of the Varuna River basin, India, using two concurrent methods of MCDM. Environment, Development and Sustainability 23, 17558-17589.

Diakoulaki, D., Mavrotas, G., Papayannakis, L., 1995. Determining Objective Weights in Multiple Criteria Problems: The Critic Method. Comput. Oper. Res. 22, 763–770. https://doi.org/10.1016/0305-0548(94)00059-H.

Dimkić, D., Dimkić, M., Vujasinović, S., 2021. Drought and alluvial groundwater resources. In Alluvial Aquifer Processes (pp. 573-665). IWA Publishing. https://doi.org/10.2166/9781789060904_0573.

Egbeyale, G.B., Ogunseye, T.T., Ozegin, K.O., 2019. Geophysical Investigation of Building Foundation in Parts of Ilorin, Kwara state using Electrical Resistivity Method. IOP Conf. Series: Journal of Physics: Conf. Series 1299 (2019), 012064. https://doi.org/10.1088/1742-6596/1299/1/012064.

Elubid, B.A., Huang, T., Peng, D.P., Ahmed, E.H., Babiker, M.M., 2020. Delineation of groundwater potential zones using integrated remote sensing, GIS and multi-criteria decision making (MCDM). Desalination and Water Treatment 192, 248-258.

Wall Emerson, R. (2023). Mann-Whitney U test and t-test. *Journal of Visual Impairment & Blindness*, *117*(1), 99-100.

Eslami, V., Ashofteh, P.S., Golfam, P., Loáiciga, H.A., 2021. Multi-criteria decision-making approach for environmental impact assessment to reduce the adverse effects of dams. Water Resources Management 35(12), 4085-4110.

Eslamian, S., Dalezios, N. R., Singh, V.P., Adamowski, J., Mohammadifard, S., Bahmani, R., ..., Namdi, A., 2017. Drought Management: Current Challenges and Future Outlook. In Handbook of Drought and Water Scarcity (pp. 729-763). CRC Press.

Ettazarini, S., El Jakani, M., 2020. Mapping of groundwater potentiality in fractured aquifers using remote sensing and GIS techniques: the case of Tafraoute region, Morocco. Environmental Earth Sciences, 79(5), 105.

Eze, S.U., Abolarin, M.O., Ozegin, K.O., Bello, M.A., William, S.J., 2021. Numerical modeling of 2-D and 3-D geoelectrical resistivity data for engineering site investigation and groundwater flow direction study in a Sedimentary terrain. Model. Earth Syst. Environ. 8(3), 3737–3755. https://doi.org/10.1007/s40808-021-01325-y.

Fajemilo, P.T., Ozegin, K.O., 2025. Evaluation of the groundwater potential of Ogbomoso, Southwestern Nigeria, using an adaptive neuro-fuzzy inference system optimized by three metaheuristic algorithms. Iran J Geophys. 8 (6), 47-78. https://doi.org/10.30499/ijg.2024.431927.1559.

Falcon, W.P., Naylor, R.L., Shankar, N.D., 2022. Rethinking global food demand for 2050. Population and Development Review 48(4), 921-957.

Fallatah, O.A., Ahmed, M., Cardace, D., Boving, T., Akanda, A.S., 2019. Assessment of modern recharge to arid region aquifers using an integrated geophysical, geochemical, and remote sensing approach. Journal of Hydrology 569, 600-611.

Farzin, M., Avand, M., Ahmadzadeh, H., Zelenakova, M., Tiefenbacher, J. P., 2021. Assessment of ensemble models for groundwater potential modeling and prediction in a karst watershed. Water 13(18), 2540.

Gaber, A., Mohamed, A.K., ElGalladi, A., Abdelkareem, M., Beshr, A.M., Koch, M., 2020. Mapping the groundwater potentiality of West Qena Area, Egypt, using integrated remote sensing and hydro-geophysical techniques. Remote Sensing, 12(10), 1559.

George, N.J., Bassey, N.E., Ekanem, A.M., Thomas, J.E., 2020. Effects of anisotropic changes on the conductivity of sedimentary aquifers, southeastern Niger Delta, Nigeria. Acta Geophysica 68(6), 1833-1843.

Ghosh, D., & Chatterjee, N. D. (2022). *Evaluation of groundwater potential using multi-criteria decision analysis and machine learning techniques. Environmental Earth Sciences*, 81(12), 322.

Giller, K.E., Delaune, T., Silva, J.V., Descheemaeker, K., van de Ven, G., Schut, A.G. ..., van Ittersum, M.K., 2021. The future of farming: Who will produce our food? Food Security 13(5), 1073-1099.

Hasan, M., Shang, Y., Akhter, G., Jin, W., 2018. Geophysical assessment of groundwater potential: a case study from Mian Channu Area, Pakistan. Groundwater 56(5), 783-796.

Hasan, M., Shang, Y., Akhter, G., Khan, M., 2017. Geophysical investigation of fresh-saline water interface: A case study from South Punjab, Pakistan. Groundwater 12527. https://doi.org/10.1111/gwat.12527.

Hashemkhani Zolfani, S., 2024. Objective weighting in MCDM: A comparative study of critic, itara, merec, and beyond. Decision Making and Artificial Intelligence Trends 1(1), 105-120.

Hassan, I., Alhamrouni, I., Azhan, N.H., 2023. A CRITIC–TOPSIS Multi-Criteria Decision-Making Approach for Optimum Site Selection for Solar PV Farm. Energies, 16(10), 4245. https://doi.org/10.3390/en16104245.

Idiahi, E., Adiat, K.A.N., Ozegin, K.O., Salufu, S.O., Adebayo, S., Akinlalu, A.A., 2023. The Assessment of Groundwater Availability in Sedimentary Environments Using the Electrical Resistivity Method: A Case of Ekpoma and Its Environs, Southern Nigeria. Indonesian Journal of Earth Sciences 3(2), A784. https://doi.org/10.52562/injoes.2023.784.

Idris, M.A., Garba, M.L., Kasim, S.A., Madabo, I. M., Dandago, K.A., 2018. The role of geological structures on groundwater occurrence and flow in crystalline basement aquifers: A status review. Bayero Journal of Pure and Applied Sciences 11(1), 155-164.

Ikpe, E.O., Ekanem, A.M., George, N.J., 2022. Modelling and assessing the protectivity of hydrogeological units using primary and secondary geo-electric indices: a case study of Ikot Ekpene Urban and its environs, southern Nigeria. Model Earth Syst Environ. https://doi.org/10.1007/s40808-022-01366-x.

Ilugbo, S.O., Aigbedion, I., Ozegin, K.O., Bawallah, M.A., 2023a. Assessment of groundwater occurrence in a typical schist belt region in Osun state, southwestern Nigeria using VES, aeromagnetic dataset, remotely sensed data and MCDA approaches. Sustain. Water Resourc. Manag. 9, 29. https://doi.org/10.1007/s40899-022-00810-1.

Ilugbo, S.O., Aigbedion, I., Ozegin, K.O., 2023b. Structural mapping for groundwater occurrence using remote sensing and geophysical data in Ilesha Schist Belt, Southwestern Nigeria. Geology, Ecology, and Landscapes. https://doi.org/10.1080/24749508.2023.2182063.

Iluore, K., Lu, J., Ozegin, K.O., 2025. Ionospheric GPS-VTEC forecasting using a hybrid deep learning model (LSTM-CNN). The Journal of Space Safety Engineering. 12, 83-93. https://doi.org/10.1016/j.jsse.2024.11.004.

Imeokparia, E.G., Falowo, O.O., 2020. Subsoil Foundation Support Assessment in Owo Area of Ondo State, Southwestern Nigeria. Geotechnical and Geological Engineering 38(2), 2009-2026.

Jitta, M.R., Radhakrishnan, S., Manda, V.K., 2025. Applications of Classical, Pairwise, and Hierarchical MCDM Techniques in Marketing Management. In Multiple-Criteria Decision-Making (MCDM) Techniques and Statistics in Marketing. IGI Global Scientific Publishing 49-74.

Kamali M.E., Naghibi, S.A., Hashemi, H., Berndtsson, R., 2020. Application of advanced machine learning algorithms to assess groundwater potential using remote sensing-derived data. Remote Sensing, 12(17), 2742.

Kanagaraj, G., Suganthi, S., Elango, L., Magesh, N.S., 2019. Assessment of groundwater potential zones in Vellore district, Tamil Nadu, India using geospatial techniques. Earth Science Informatics 12, 211-223.

Karakuş, C.B., 2023. Groundwater potential assessment based on GIS-based best–worst method (BWM) and step-wise weight assessment ratio analysis (SWARA) method. Environmental science and pollution research 30(11), 31851-31880. https://doi.org/10.1007/s11356-022-24425-3.

Khalil, U., Imtiaz, I., Aslam, B., Ullah, I., Tariq, A., Qin, S., 2022. Comparative analysis of machine learning and multi-criteria decision-making techniques for landslide susceptibility mapping of Muzaffarabad district. Frontiers in Environmental Science 10, 1028373.

Konwea, C.I., Evurani, D.E., Ajayi, O., 2023. Assessment of groundwater potential of the Obafemi Awolowo University Estate, Southwestern Nigeria. Scientific African 20, e01597.

Kuruppu, U., Rahman, A., & Rahman, M. A. (2019). Permeable pavement as a stormwater best management practice: a review and discussion. Environmental Earth Sciences, 78, 1-20.

Liaqat, M. U., Mohamed, M. M., Chowdhury, R., Elmahdy, S. I., Khan, Q., & Ansari, R. (2021). Impact of land use/land cover changes on groundwater resources in Al Ain region of the United Arab Emirates using remote sensing and GIS techniques. Groundwater for Sustainable Development, 14, 100587.

Loke, M.H. and Barker, R.D., 1996, Rapid least-squares inversion of apparent resistivity pseudo sections by a quasi-Newton method. Geophysical Prospecting, 44, 131–152. https://doi.org/10.1111/j.1365-2478.1996.tb00142.x

Luo, Y., Zhang, X., Qin, Y., Yang, Z., Liang, Y., 2021. Tourism attraction selection with sentiment analysis of online reviews based on probabilistic linguistic term sets and the IDOCRIW-COCOSO model. International Journal of Fuzzy Systems 23, 295-308.

Magdoff, F., Williams, C., 2017. Creating an ecological society: toward a revolutionary transformation. NYU Press.

Mahato, A., Upadhyay, S., & Sharma, D., 2022. Global water scarcity due to climate change and its conservation strategies with special reference to India: a review. Plant Archives (09725210), 22(1).

Maity, D.K., Mandal, S., 2019. Identification of groundwater potential zones of the Kumari River basin, India: an RS & GIS based semi-quantitative approach. Environment, Development and Sustainability 21, 1013-1034.

Maliva, R.G., 2016. Aquifer characterization techniques. Schlumberger Methods in Water Resources Evaluation Series 4. Springer Hydrogeology. https://doi.org/10.1007/978-3-319-32137-0.

Mallick, J., Khan, R.A., Ahmed, M., Alqadhi, S.D., Alsubih, M., Falqi, I., Hasan, M.A., 2019. Modeling groundwater potential zone in a semi-arid region of Aseer using fuzzy-AHP and geoinformation techniques. Water, 11(12), 2656.

Masroor, M., Sajjad, H., Kumar, P., Saha, T.K., Rahaman, M.H., Choudhari, P., Kulimushi, L.C., Pal, S., Saito, O., 2023. Novel ensemble machine learning modeling approach for groundwater potential mapping in Parbhani District of Maharashtra, India. Water 15 (3), 419. https://doi.org/10.3390/w15030419.

Mogaji, K.A., Atenidegbe, O.F., 2023. Development of PROMETHEE-Entropy data mining model for groundwater potentiality modeling: a case study of multifaceted geologic settings in south-western Nigeria. Acta Geophysica 1-28.

Mogaji, K.A., Lim, H.S., 2017. Application of a GIS-/remote sensing-based approach for predicting groundwater potential zones using a multi-criteria data mining methodology. Environmental Monitoring and Assessment 189, 1-26.

Mogaji, K.A., Omobude, O.B., 2017. Modeling of geoelectric parameters for assessing groundwater potentiality in a multifaceted geologic terrain, Ipinsa Southwest, Nigeria–A GIS-based GODT approach. NRIAG Journal of Astronomy and Geophysics 6(2), 434-451.

Mogaji, K.A., Atenidegbe, O.F., Adeyemo, I.A., Akinmulewo, K P., 2022. Application of GIS-based PROMETHEE data mining technique to geoelectrical-derived parameters for aquifer potentiality assessment in a typical hardrock terrain Southwestern Nigeria. Sustainable Water Resources Management 8(2), 51.

Mogaji, K.A., Ezekiel, G.I., Abodunde, O.O., 2021. Modeling of aquifer potentiality using GIS-based knowledge-driven technique: a case study of hard rock geological setting, southwestern Nigeria. Sustainable Water Resources Management 7(4), 64.

Mokadem, N., Boughariou, E., Mudarra, M., Brahim, F.B., Andreo, B., Hamed, Y., Bouri, S., 2018. Mapping potential zones for groundwater recharge and its evaluation in arid environments using a GIS approach: case study of North Gafsa Basin (Central Tunisia). Journal of African Earth Sciences 141, 107-117.

Mpofu, M., Madi, K., Gwavava, O., 2020. Remote sensing, geological, and geophysical investigation in the area of Ndlambe Municipality, Eastern Cape Province, South Africa: Implications for groundwater potential. Groundwater for Sustainable Development 11, 100431.

Mudashiru, S.A., Olatunji, A. O., Oke, P.A., Adeyanju, O. L., Orowale T.P., 2024. Subsurface Competence Evaluation Using Electrical Resistivity Method at a Proposed Building Site Along Futa Staff Quarters, Oba Nla, Aku re Southwestern Nigeria. Pakistan Journal of Geology 6(2), 80.87.

Nag, S., Roy, M. B., Roy, P.K., 2022. Study on the functionality of land use land cover over the evaluation of groundwater potential zone: A fuzzy AHP based approach. Journal of Earth System Science 131(3), 146.

Nair, A.M., Prasad, K.R., Srinivas, R., 2022. Groundwater vulnerability assessment of an urban coastal phreatic aquifer in India using GIS-based DRASTIC model. Groundwater for Sustainable Development 19, 100810.

Odukoya, A.M. 2015. Geochemical and quality assessment of groundwater in some Nigerian basement complex. International journal of environmental science and technology 12, 3643-3656

Ojo, J.S., Olorunfemi, M.O., Bayode, S., Akintorinwa, O.J., Omosuyi, G.O., Akinluyi, F. O., 2014. Constraint map for landfill site selection in Akure Metropolis, Southwestern Nigeria. Ife journal of science 16(3), 405-416

Olajide, A., Bayode, S., Fagbemigun, T., Oyebamiji, A., Amosun, J. and Owasanoye, A., 2020. Evaluation of aquifer protective capacity and groundwater potential in part of Iju, Akure-North, Ondo State, Nigeria. Journal of the Nigerian society of Physical Sciences 197-204.

Omonijo, A.G. and Matzarakis, A., 2011. Climate and bioclimate analysis of Ondo State, Nigeria. Meteorologische Zeitschrift, 20(5), p.531.

Omosuyi, G.O., Oshodi, D.R., Sanusi, S.O., Adeyemo, I.A., 2021. Groundwater potential evaluation using geoelectrical and analytical hierarchy process modeling techniques in Akure-Owode, southwestern Nigeria. Modeling Earth Systems and Environment 7, 145-158.

Osinowo, O.O., Arowoogun, K.I., 2020. A multi-criteria decision analysis for groundwater potential evaluation in parts of Ibadan, southwestern Nigeria. Applied Water Science, 10(11), 228

Osinowo, O. O., & Arowoogun, K. I. (2020). A multi-criteria decision analysis for groundwater potential evaluation in parts of Ibadan, southwestern Nigeria. Applied Water Science, 10(11), 228

Ozegin, K.O., Ilugbo, S.O., 2025. Evaluation of potentially susceptible flooding areas leveraging geospatial technology with multicriteria decision analysis in Edo State, Nigeria. Natural Hazards Research 5(1), 109-133. https://doi.org/10.1016/j.nhres.2024.07.002

Ozegin, K.O., Ilugbo, S.O., Ogunseye, T.T., 2023. Groundwater exploration in a landscape with heterogeneous geology: an application of geospatial and analytical hierarchical process (AHP) techniques in the Edo north region, in Nigeria. Groundwater for Sustainable Development 20, 100871. https://doi.org/10.1016/j.gsd.2022.100871.

Ozegin, K.O., Ilugbo, S.O., Adebo, B., 2024a. Spatial evaluation of groundwater vulnerability using the DRASTIC-L model with the analytic hierarchy process (AHP) and GIS approaches in Edo State, Nigeria. Phys. Chem. Earth 134, 103562. https://doi.org/10.1016/j.pce.2024.103562.

Ozegin, K.O., Ilugbo, S.O., Akande, O.N., 2024b. Leveraging geospatial technology and AHP for groundwater potential zonation in parts of south and north-Central Nigeria. Sustainable Water Resources Management. 10, 146. https://doi.org/10.1007/s40899-024-01124-0.

Ozegin, K.O., Ilugbo, S.O., Alile, O.M., Iluore, K., 2024c. Integrating in-situ data and spatial decision support systems (SDSS) to identify groundwater potential sites in the Esan plateau, Nigeria. Groundwater for Sustainable Development 26, 101276. https://doi.org/10.1016/j.gsd.2024.101276.

Pal, S.C., Ghosh, C., Chowdhuri, I., 2020. Assessment of groundwater potentiality using geospatial techniques in Purba Bardhaman district, West Bengal. Applied Water Science 10(10), 221.

Panahi, M. R., Mousavi, S. M., Rahimzadegan, M., 2017. Delineation of groundwater potential zones using remote sensing, GIS, and AHP technique in Tehran–Karaj plain, Iran. Environmental earth sciences 76, 1-15.

Pathan, A.I., Agnihotri, P.G., Patel, D., 2022. Integrated approach of AHP and TOPSIS (MCDM) techniques with GIS for dam site suitability mapping: a case study of Navsari City, Gujarat, India. Environmental Earth Sciences 81(18), 443.

Paul, R.S., Rawat, U., SenGupta, D., Biswas, A., Tripathi, S., Ghosh, P., 2020. Assessment of groundwater potential zones using multi-criteria evaluation technique of Paisuni river basin from the combined state of Uttar Pradesh and Madhya Pradesh, India. Environmental Earth Sciences 79 (13), 1-24. https://doi.org/10.1007/s12665-020-09091-3.

Pena, M.A.C., de Paula, R.S., Velasquez, L.N.M., Neto, W.M.P., 2024. Estimating transmissivity and storativity in a karst aquifer by direct and indirect methods. Hydrological Processes, 38(4), e15116.

Petrović, G., Mihajlović, J., Marković, D., Hashemkhani Zolfani, S., Madić, M., 2023. Comparison of aggregation operators in the group decision-making process: A real case study of location selection problem. Sustainability 15(10), 8229.

Popović, M., 2021. A MCDM approach for personnel selection using the COCOSO method. Journal of Process Management and New Technologies. www.japmnt.com ISSN: 2334-735X (Print) ISSN: 2334-7449 (Online)

Pramanik, P. K. D., Biswas, S., Pal, S., Marinković, D., & Choudhury, P. (2021). A comparative analysis of multi-criteria decision-making methods for resource selection in mobile crowd computing. *Symmetry*, *13*(9), 1713.

Radulović, M., Brdar, S., Mesaroš, M., Lukić, T., Savić, S., Basarin, B., & Pavić, D., 2022. Assessment of groundwater potential zones using GIS and fuzzy AHP techniques—a case study of the Titel municipality (Northern Serbia). ISPRS International Journal of Geo-Information, 11(4), 257.

Rahman, K. U., Hussain, A., Ejaz, N., Shahid, M., Duan, Z., Mohammadi, B., Anh, D. T. 2022. Evaluating the impact of the environment on depleting groundwater resources: a case study from a semi-arid and arid climatic region. Hydrological Sciences Journal 67(5), 791-805.

Rasoanaivo, R., Zaraté, P., 2024. SAGeLogE: A Decision Support System for Students' Accommodation Management. Journal of Computer and Communications. 12, 107-145. https://doi.org/10.4236/jcc.2024.123008.

Robinson, N. P., Allred, B. W., Jones, M. O., Moreno, A., Kimball, J. S., Naugle, D. E., Richardson, A. D., 2017. A dynamic Landsat derived normalized difference vegetation index (NDVI) product for the conterminous United States. Remote sensing 9(8), 863.

Roozbahani, A., Ebrahimi, E., Banihabib, M. E., 2017. Ground water risk management using dynamic bayesian networks and PROMETHEE method. In Proceedings of the 10th World Congress of EWRA 'PantaRhei', Athens.

Roszkowska, E., 2013. Rank Ordering Criteria Weighting Methods—A Comparative Overview. Optimum. Econ. Stud. 65, 14–33. https://doi.org/10.15290/ose.2013.05.65.02

Şahin, M., 2021. A comprehensive analysis of weighting and multicriteria methods in the context of sustainable energy. International Journal of Environmental Science and Technology 18(6), 1591-1616.

Sahoo, S.K., Goswami, S.S., 2023. A comprehensive review of multiple criteria decision-making (MCDM) methods: advancements, applications, and future directions. Decision Making Advances 1(1), 25-48.

Scanlon, B. R., Fakhreddine, S., Rateb, A., de Graaf, I., Famiglietti, J., Gleeson, T., Zheng, C., 2023. Global water resources and the role of groundwater in a resilient water future. Nature Reviews Earth & Environment, 4(2), 87-101.

Shi, H., Li, Y., Jiang, Z., Zhang, J., 2021. Comprehensive power quality evaluation method of microgrid with dynamic weighting based on CRITIC. Measurement and Control, 54(5-6), 1097-1104.

Shishaye, H. A., Abdi, S., 2016. Groundwater exploration for water well site locations using geophysical survey methods. Hydrol. Curr. Res, 7(1).

Singh, M., Pant, M., 2021. A review of selected weighing methods in MCDM with a case study. International Journal of System Assurance Engineering and Management 12(1), 126-144.

Stojanovic, I., Puška, A., Selakovic, M., 2022. A Multi-Criteria Approach to the Comparative Analysis of the Global Innovation Index on the Example of the Western Balkan Countries. Economics-Innov. Econ. Res. J. 10, 9–26. https://doi.org/10.2478/eoik-2022-0019.

Trinkuniene, E., Podvezko, V., Zavadskas, E. K., Joksiene, I., Vinogradova, I., Trinkunas, V., 2017. Evaluation of quality assurance in contractor contracts by multi-attribute decision-making methods. Economic Research (Ekonomska Istrazivanja), 30(1), 1152–1180.150.

Tsur, Y., 2018. The stabilization role of groundwater when surface water supplies are uncertain: The implications for groundwater development. In Economics of Water Resources (pp. 209-216). Routledge.

Vinogradova, I., Podvezko, V., Zavadskas, E. K., 2018. The recalculation of the weights of criteria in MCDM methods using the bayes approach. Symmetry, 10(6), 1–18.

Wada, Y., 2016. Modeling groundwater depletion at regional and global scales: Present state and future prospects. Surveys in Geophysics, 37(2), 419-451.

Waltz, J.P., 2019. Ground water. In Introduction to physical hydrology (pp. 122-130). Routledge.

Yazdani, M., Zaraté, P., Kazimieras Zavadskas, E. and Turskis, Z. (2019) A Combined Compromise Solution (CoCoSo) Method for Multi-Criteria Decision-Making Problems. Management Decision, 57, 2501-2519. https://doi.org/10.1108/MD-05-2017-0458.

Zavadskas, E.K., Podvezko, V., 2016. Integrated determination of objective criteria weights in MCDM. International Journal of Information Technology & Decision Making 15(02), 267-283.

Zavadskas, E. K., Cavallaro, F., Podvezko, V., Ubarte, I., Kaklauskas, A., 2017. MCDM Assessment of a Healthy and Safe Built Environment According to Sustainable Development Principles: A Practical Neighborhood Approach in Vilnius. Sustainability 9(5), 702. https://doi.org/10.3390/su9050702.

Zhang, W., & Jiang, J. (2024). Bootstrap-based resampling methods for software reliability measurement under small sample condition. *Journal of Circuits, Systems and Computers*, *33*(09), 2450161.

Zhu, C., Lin, Y., Zhang, J., Gan, M., Xu, H., Li, W., Yuan, S., Wang, K., 2021. Exploring the relationship between rural transition and agricultural eco-environment using a coupling analysis: A case study of Zhejiang Province, China. Ecological Indicators. 127, 107733. https://doi.org/10.1016/j.ecolind.2021.107733.